TOR signaling is required for host lipid metabolic remodelling and survival following enteric infection in *Drosophila*

Rujuta Deshpande, Byoungchun Lee, Yuemeng Qiao and Savraj S Grewal*

Clark H Smith Brain Tumour Centre, Arnie Charbonneau Cancer Institute, Alberta Children's Hospital Research Institute, and Department of Biochemistry and Molecular Biology Calgary, University of Calgary, Alberta T2N 4N1, Canada.

*Author for correspondence (grewalss@ucalgary.ca)

SUMMARY

When infected by enteric pathogenic bacteria, animals need to initiate local and whole-body defence strategies. While most attention has focused on the role innate immune anti-bacterial responses, less is known about how changes in host metabolism contribute to host defence. Using *Drosophila* as a model system, we identify induction of intestinal target-of-rapamycin (TOR) kinase signaling as a key adaptive metabolic response to enteric infection. We find that enteric infection induces both local and systemic induction of TOR independently of the IMD innate immune pathway, and we see that TOR functions together with IMD signaling to promote infection survival. These protective effects of TOR signaling are associated with re-modelling of host lipid metabolism. Thus, we see that TOR is required to limit excessive infection-mediated wasting of host lipid stores by promoting an increase in the levels of gut- and fat body-expressed lipid synthesis genes. Our data supports a model in which induction of TOR represents a host tolerance response to counteract infection-mediated lipid wasting in order to promote survival.

INTRODUCTION

A central role for the immune system is to sense invading bacterial pathogens and then trigger appropriate defence responses. One defence strategy is to decrease pathogen load (Schneider and Ayres, 2008). Central to this mechanism are the innate immune responses. These are responsible for sensing invading bacteria at the sites of infection and then activating both local and whole-body

© 2022. Published by The Company of Biologists Ltd.
This is an Open Access article distributed under the terms of the Creative Commons Attribution License (http://creativecommons.org/licenses/by/4.0), which permits unrestricted use, distribution and reproduction in any medium provided that the original work is properly attributed.

Disease Models & Mechanisms • DMM • Accepted manuscript

host anti-bacterial responses (Buchon et al., 2014). It also becoming clear that changes in host metabolism are another important defence strategy against infection (Ayres and Schneider, 2012; Medzhitov et al., 2012; Troha and Ayres, 2020). The innate immune response can be energetically costly, and these metabolic changes are often needed to fuel the immune response (Krejcova et al., 2019; Man et al., 2017). In addition, metabolic reprogramming is often essential for animals to adapt to and tolerate the presence of pathogens (Ganeshan et al., 2019; Sanchez et al., 2018; Wang et al., 2018; Wang et al., 2016; Weis et al., 2017). Indeed, there is increasing appreciation that for a given pathogen load, inter-individual differences in survival outcomes are determined by differences in the ability to mediate appropriate metabolic adaptations to infection (Troha and Ayres, 2020). However, compared to our understanding of innate immunity, less is known, about how these metabolic adaptations promote host fitness upon infection.

Drosophila has provided a powerful model system to study host defence responses to enteric bacterial infection (Buchon *et al.*, 2014; Lee and Lee, 2018). Upon ingestion of pathogenic bacteria, the intestine triggers two main responses to mount antibacterial defenses. The first involves activation of the conserved IMD/Relish/NF-KappaB pathway by Gram-negative bacteria, which leads to production of antimicrobial peptides (AMPs) (Buchon *et al.*, 2014). The second involves bacteria-derived uracil, which stimulates reactive oxygen species (ROS) production in intestinal epithelial cells (Lee et al., 2018; Lee et al., 2015). Both pathways can promote local antimicrobial responses in the intestine and also trigger signaling from the intestine to other tissues to promote whole-body anti-bacterial response such as production of AMPs from the fat body (Wu et al., 2012; Yang et al., 2019). Enteric infection can also alter both intestinal and whole-body metabolism, but the contributions of these effects to defence against pathogens are not fully clear (Galenza and Foley, 2019; Lee and Lee, 2018; Wong et al., 2016).

TOR kinase is a conserved regulator of cell, tissue and whole-body metabolism (Ben-Sahra and Manning, 2017; Howell et al., 2013; Saxton and Sabatini, 2017). In general, TOR is activated under favourable conditions (e.g. growth factor stimulation and nutrient availability) to stimulate cellular anabolic metabolism and promote growth. In contrast, under stress conditions such as starvation, hypoxia or oxidative damage, TOR is inhibited to promote catabolic metabolism to ensure cell survival. The utility of *Drosophila* genetics has also been instrumental in showing how TOR activation in specific tissues can trigger and coordinate whole body-level physiological and metabolic responses (Boulan et al., 2015; Grewal, 2009; Texada et al., 2020). These effects rely on

Disease Models & Mechanisms • DMM • Accepted manuscript

the ability of TOR signaling to promote inter-organ communication and endocrine signaling and have been shown to be essential for organismal responses to environmental changes such as altered nutrition and hypoxia (Boulan *et al.*, 2015; Koyama et al., 2020).

Given the central role for TOR in controlling whole-body physiology and metabolism, some studies have begun to explore its role in responses to bacterial infection in *Drosophila*. However, these studies have differed in their conclusions about whether TOR activity is helpful or harmful to host immune responses and fitness upon infection. In some cases, it was reported that reduced TOR activity provided a benefit to the host. For example, enteric infection with *Ecc15*, a Gram-negative bacterium, was shown to inhibit TOR and lead to increased lipid breakdown in the gut (Lee *et al.*, 2018). This loss-of-TOR mediated metabolic shift to lipid catabolism was required for the antimicrobial ROS response and increased the host resistance to enteric infection. Similarly, another report showed that lowered TOR activity upon enteric infection could induce AMPs (Varma et al., 2014). Finally, one report showed that lowering TOR activity, either genetically or by nutrient restriction, was sufficient to increase survival upon systemic infection with either *P. aeruginosa* or *S. aureus* (Lee et al., 2017*)*. In contrast to these findings, other studies showed that lowered TOR activity is detrimental to hosts upon infection. For example, enteric infection with, *P.entomophila* decreased gut TOR activity, leading to suppressed intestinal protein synthesis, which reduced immune responses and prevented proper intestinal tissue repair (Chakrabarti et al., 2012). Another study also showed that TOR inhibition reduced fly survival upon systemic infection with *B. Cepacia* (Allen et al., 2016). The reasons for these differences in the links between TOR and infection response in *Drosophila* may be due to the different bacterial infections used or because of differences in host metabolic or nutrient status. Nevertheless, they indicate that further work is required to clarify how TOR may play a role in immune and metabolic responses to infection. We address this issue in this paper. We show that enteric infection leads to increased TOR signaling independently of innate signaling, and that this induction is required to remodel host lipid metabolism and promote survival.

Disease Models & Mechanisms • DMM • Accepted manuscript

RESULTS

Enteric bacterial infection stimulates local and systemic TOR signaling

TOR kinase couples environmental signals to changes in cellular metabolism. Generally, TOR has been shown to be activated by favorable conditions (e.g., abundance of nutrients and growth factors), while being inhibited by stress conditions (e.g., starvation, low oxygen, oxidative stress). We were interested in examining how TOR activity might be affected by enteric bacterial infection. We first infected flies with the Gram-negative bacteria *Pseudomonas entomophila (P.e)* for 4hr and then dissected intestines for western blotting. At this time point following feeding, *P.e.* is able to colonize fly intestines as previously described (Figure S1A). Ribosomal protein S6 kinase (S6K), is directly phosphorylated and activated by TOR, hence we used western blotting for phosphorylated S6K as a readout for TOR activity. We found that oral *P.e.* feeding led to increased phosphorylated S6K levels (Figure 1A). This increase was blocked by pre-feeding the flies rapamycin, a TOR inhibitor, indicating that the induction of phosphorylated S6K was through an increase in TOR activity (Figure S1B). We also examined phosphorylation of ribosomal protein S6, a downstream target of ribosomal protein S6 kinase, and we saw that 4hrs of oral *P.e* infection also induced phosphorylated S6 levels in the intestine (Figure 1B). When we performed immunostaining with the anti-phosphorylated S6 antibody, we also saw an increase in TOR activity particularly in the anterior region of the midgut ((Figure S1C). The increased phosphorylated S6 staining was seen in GFP-marked stem cells/EB cells, consistent with a previous report that showed that enteric infection induces TOR signaling in intestinal stem cells (Haller et al., 2017). However, we also saw phosphorylated S6 staining in the surrounding large polyploid GFP-negative cells, which are likely the enterocyte epithelial cells (Figure S1D). A conserved function of TOR is the stimulation of cellular protein synthetic capacity, in large part mediated via upregulation of tRNA and rRNAs, and genes involved in ribosome synthesis (Ghosh et al., 2014; Killip and Grewal, 2012; Marshall et al., 2012; Mayer and Grummt, 2006; Rideout et al., 2012). When we used qRT- PCR to measure RNA levels in intestinal samples, we saw that oral *P.e*. infection led to an increase in tRNA and pre-rRNA levels and an increase in mRNA levels of three ribosome biogenesis genes, *Nop5, ppan, fibrillarin* upon oral *P.e* infection (Figure S1E). We explored the effects of oral bacterial infection further by performing a time course following oral *P.e.* feeding. We saw that the induction of TOR was rapid (within 4hrs of infection) and persisted for 24hrs of the oral infection period (Figure S2A). We also found that this induction of TOR was similar in males and females (Figure S2B). Moreover, the effects of *P.e*. appear limited to adults since 4hr oral infection in larvae didn't increase

Disease Models & Mechanisms • DMM • Accepted manuscript

phosphorylated S6K levels, and in fact showed a small decrease (Figure S2C). We also tested two other pathogenic Gram-negative bacteria, *Vibrio cholera (V.c.)* and *Erwinia carotovora carotovora (Ecc15*). We again used western blotting for phosphorylated S6K to measure TOR and saw that oral infection with *V.c.* and *Ecc15* both led to increased intestinal TOR activity (Figure S2D). Together, these data indicate that induction of intestinal TOR kinase signaling is a rapid response to enteric Gram-negative bacterial infection.

As well as affecting intestinal physiology, enteric infection can also trigger non-autonomous, systemic responses that can impact physiology in remote tissues. We therefore examined whether enteric infection might induce TOR activity more widely. We found that oral *P.e.* feeding lead to increased phosphorylated S6K levels in both whole animals and in isolated abdomens, which are enriched in fat body, a tissue in which TOR plays important roles in the control of organismal metabolism and physiology (Figure 1C, D). These results suggest that enteric bacterial infection can lead to non-autonomous induction of TOR in other metabolically important tissues. One main way that systemic TOR activity can be controlled is through the endocrine insulin signaling pathway. In *Drosophila*, seven insulin-like peptides (dILPs) are secreted into the hemolymph from the brain and other tissues where they can function in a long-range manner to activate a conserved PI3K/Akt kinase signaling pathway in target tissues. Activated Akt can signal by stimulating TOR or by blocking the nuclear localization and activity of the FOXO transcription factor. We therefore explored whether enteric infection might mediate non-autonomous induction of TOR signaling by upregulating systemic insulin signaling. We first measured phosphorylation of Akt as a read-out of insulin signaling. We found that following oral infection with *P.e.* there was an increase in Akt phosphorylation in both whole animal samples and isolated abdominal tissues samples (Figure 1C, D, Figure S3B, C), suggesting an increase systemic insulin signaling. Interestingly, this increase in Akt phosphorylation was not seen in the intestine following oral infection with *P.e.* (Figure S3A). We also measured mRNA levels of 4EBP, a FOXO target gene. We found that oral *P.e.* infection was sufficient to reduce 4EBP levels in both whole-animal and isolated abdominal samples (Figure 1E, F), which is also consistent with elevated insulin signaling. One main way that insulin signaling can be induced is through increased production of the dILPs. We found that *P.e.* infection was sufficient to increase expression of three dILPs (dILP3,5 and 7) (Figure 1G). To test if this increase in insulin signaling could explain the induction of systemic TOR signaling upon infection, we examined the effects of overexpression of ImpL2, the *Drosophila* homolog of the mammalian insulin-like growth factor binding protein. ImpL2 binds to dILPs and inhibits their ability to signal through the insulin

Disease Models & Mechanisms • DMM • Accepted manuscript

receptor. We found that ubiquitous overexpression of ImpL2 was sufficient to block insulin signaling (as measured by Akt phosphorylation) (Figure 1H) and to prevent that infection-mediated increase in TOR signaling, as measured by S6K phosphorylation (Figure 1H). Together, these data suggest that enteric infection can induce direct stimulation of intestinal TOR activity and also a non-autonomous upregulation of whole-body insulin/TOR signaling.

We next explored whether other enteric intestine stresses might also regulate TOR signaling. Feeding flies with three known chemical intestine stressors, bleomycin (a DNA damaging agent), dextran sodium sulphate (DSS, a detergent) and paraquat (an oxidative stressor), had no effect on intestinal TOR activity (Figure S4A). We also explored two nutrient stresses - high sugar and high fat. However, we saw that feeding the flies either a high sugar (40%) or high fat (30%) supplemented diet, also did not have any effect on TOR signaling in the intestine (Figure S4B). Together our data suggests that the induction of TOR appears specific to oral bacterial infection. Interestingly this induction occurs in a bacterial concentration-manner and is seen by low levels of bacterial infection (Figure S4C).

Infection-mediated TOR stimulation is independent of IMD and ROS signaling.

A primary and well-studied response to enteric Gram-negative bacterial infection is activation of the Immune deficiency (IMD)/ NF-kB pathway (Kleino and Silverman, 2014). We therefore examined whether either increased IMD signaling might be the trigger for TOR induction upon oral *P.e.* infection. We began by examining mutants for *imd,* a death domain containing protein that is a key effector of the IMD signaling cascade. We infected either control (w^{1118}) or *imd* mutants with *P.e.* and saw that the induction of AMPs was completely suppressed in the *imd* mutants, confirming that they are impaired in proper immune signaling (Figure S5). However, when we examined TOR activity by measuring S6K phosphorylation by western blot, we found that infection-induced increase in TOR activity both in the intestine and whole animal was unaffected in *imd* mutants (Figure 2A-C). We also examined mutants for the NF-κB-like transcription factor, Relish, which is the downstream transcriptional effector of the IMD pathway. Again, we found that the induction of intestinal TOR upon oral *P.e* infection was still observed in the *relish* mutants (Figure 2D). These results suggest that TOR induction seen upon enteric *P.e.* infection is independent of IMD signaling.

Disease Models & Mechanisms • DMM • Accepted manuscript

Induction of reactive oxygen species (ROS) signaling by bacteria-derived uracil signaling also mediates immune responses upon enteric infection with Gram-negative bacteria (Lee *et al.*, 2015; Wu *et al.*, 2012). However, we found that feeding uracil had no effect on TOR signaling and we also found that feeding the flies N-acetylcysteine, potent antioxidant, along with oral *P.e.* feeding didn't reverse the induction of TOR upon infection (Figure S6A, B). Together with our result with paraquat, a stimulator of ROS (Figure S4A), our data suggests that TOR induction is independent of ROS.

Inhibiting TOR and IMD pathways simultaneously reduces survival upon *P.e.* infection.
We next examined the consequences of TOR induction upon *P.e.* infection. We first examined effects on survival following enteric *P.e.* infection. Under our laboratory fly culture conditions, the strain of *P.e.* we use is not strongly pathogenic. Thus, when we infected control (w^{1118}) adult flies for 2 days and then monitored their survival over approximately three weeks, we saw little effect on viability compared to uninfected flies (Figure 2E). When we infected flies and simultaneously inhibited TOR by feeding flies rapamycin, we found that this induced a slight, but significant, decrease in survival compared to flies fed rapamycin alone (Figure 2E). We next tested the possibility that TOR functions in parallel IMD/Relish signaling to promote infection survival. We found that *relish* mutants had a generally reduced lifespan on our normal lab food compared to control (w^{1118}) adults (Figure 2F). Either enteric infection with *P.e.,* or blocking TOR with rapamycin, had no effect on viability in the *relish* mutants alone. However, when we infected *relish* mutants and simultaneously fed them rapamycin to inhibit TOR, we saw a significant decrease in survival compared to *relish* mutant flies subjected to infection or rapamycin treatment alone (Figure 2F). These results suggest that in order to survive enteric infection, an animal needs cooperative activation of both IMD/Relish and TOR signaling.

A primary infection response induced by the IMD pathway in flies is the production of anti-microbial peptides (AMPs) (Kleino and Silverman, 2014). We saw that oral infection with *P.e.* led to a strong induction of several AMPs, including *Cecropin A (CecA), Cecropin C (CecC), Metchnikowin (Mtk),* and *Drosocin (Dro)* (Figure 3A-D). However, when we inhibited TOR by feeding flies rapamycin this induction was not significantly affected (Figure 3A-D). We also examined host bacterial load (as measured by colony forming units) during a 24 hour infection period and a subsequent three day recovery period. We saw that the pathogen abundance was initially high following infection and then declined at each time point and was below detection at 3 days

Disease Models & Mechanisms • DMM • Accepted manuscript

following infection (Figure 3E). We also found that bacterial load was unaffected by inhibition of TOR signaling by rapamycin at each time point (Figure 3E). These results suggest that the induction of TOR upon infection may not be required to induce antibacterial resistance responses, and that the requirement for TOR in infection survival may reflect a role in other immune responses.

TOR induction limits lipid depletion and promotes lipid synthesis upon infection.

Initiating immune responses against infection can be energetically costly for infected hosts. Remodelling of host metabolism is therefore increasingly recognized as an important component of immune responses (Troha and Ayres, 2020). Given that TOR kinase is a conserved regulator of metabolism, we investigated whether it might play a role in modulating host metabolic responses to infection. Lipid stores are an important metabolic fuel source. Lipids can be synthesized and stored as triacyglycerides (TAGs) in lipid droplets in the fly fat body, oenocytes and intestine. They can be then mobilized, transported to tissues, and used to fuel metabolism, particularly in stress conditions (Heier and Kuhnlein, 2018). We tested for changes in TAGs upon oral *P.e.* infection and found a significant decrease in infected w^{1118} adult females compared to control flies (Figure 4A) as has been reported following systemic infection in flies (Chambers et al., 2012; Dionne et al., 2006). Since the majority of the lipid stores are stored in the fat body (Zhao and Karpac, 2020), we dissected the fat bodies of infected females, and found a decrease in the lipid droplet size by BODIPY staining (Figure 4B). We also saw that enterocytes in the anterior region of the midgut accumulated lipid droplets as visualized by Oil Red O and bodipy staining (Figure 4C-E) as has been reported previously (Kamareddine et al., 2018a; Luis et al., 2016; Miguel-Aliaga et al., 2018). We found that oral infection with *P.e.* led to a depletion of these intestinal lipids(Figure 4C-E). These results suggest that infection leads to mobilization of fat body and intestinal lipid stores, perhaps as a way to provide lipids to other tissues to fuel their metabolism, as has been recently reported (Zhao and Karpac, 2021). In support of this idea, we also saw that enteric infection increased whole-body expression of two lipid binding proteins, apoLpp and Mtp, that are highly expressed in the fat body and that are needed for transport of lipids through the hemolymph (Figure S7).

We next examined what role TOR might play in these lipid effects by measuring TAG levels at 0-, 1- and 3-days following infection in control vs rapamycin-treated flies. In control flies, infection led to a transient decrease in TAG levels at the 1-day timepoint, but then TAGs recovered to the same level as uninfected flies at 3 days (Figure 4F). Rapamycin treatment alone had no significant effect on TAG levels at any timepoint compared to uninfected control flies (Figure 4F). However, when we

Disease Models & Mechanisms • DMM • Accepted manuscript

infected flies and simultaneously fed them rapamycin to inhibit TOR, we saw a progressive depletion of TAG stores at each timepoint following infection (Figure 4F).

Our results suggest TOR is needed to limit excessive loss of lipid stores post infection. To do this, TOR may be blocking excess lipase function (to limit lipolysis) or may be increasing lipid synthesis (to resupply new lipids following infection). To explore this further we examined the expression of genes required for de-novo lipid synthesis. We found that flies infected orally with *P.e.* showed a significant upregulation in mRNA expression levels of genes required for lipid synthesis such as acetyl-CoA carboxylase (ACC), fatty acid synthetase 1 (FASN1), midway (mdy/DGAT1), dgat2, lipin, and lsd2 (Figure 5A). Moreover, the expression levels of two transcription factors, SREBP and Mondo, which promote the transcription of these genes (Heier and Kuhnlein, 2018; Mattila and Hietakangas, 2017) were also upregulated (Figure 5A). In *Drosophila* adults, lipid synthesis occurs in the intestine, the fat body and oenocytes (Heier and Kuhnlein, 2018). We therefore carried out tissue-specific analysis of lipid synthesis gene expression in both intestines and isolated abdominal samples (which are enriched in fat body and oenocytes). In both cases we saw that enteric *P.e.* infection increased expression levels of lipid synthesis genes, suggesting that following infection new lipid synthesis is induced in several important lipid metabolic tissues (Figure 5B, C). To explore how TOR might be involved in these effects, we examined the effects of rapamycin feeding to inhibit TOR. We found that the *P.e.*-induced increase in expression of lipid synthesis genes and transcription factors was significantly blunted in flies that had been fed rapamycin to block TOR (Figure 6). These results suggest that one role for the increased TOR activity that we see upon infection may be to induce de novo lipid synthesis to replenish the lipid stores that are mobilized following enteric infection.

Infection promotes glycogen mobilization through TOR signaling.

De novo lipid synthesis often relies on metabolic conversion of glucose into acetyl-CoA which can then serve as the source for new TAG synthesis (Heier and Kuhnlein, 2018). Flies can acquire glucose both from their diet and also from mobilization of stored glucose in the form of glycogen (Mattila and Hietakangas, 2017). When we infected flies with *P.e.* we saw a significant decrease in whole-body glycogen levels, as has been reported following systemic infection (Chambers *et al.*, 2012; Dionne *et al.*, 2006), and an increase in mRNA expression levels of several genes required for glycogen mobilization such as glycogen phosphorylase (GlyP), AGL/ CG9485, and UDP-glucose pyrophosphorylase (UGP) (Figure 7A, B). These results indicate that infection triggers a

Disease Models & Mechanisms • DMM • Accepted manuscript

mobilization of host glycogen stores. Interestingly, when we blocked TOR signaling by feeding flies rapamycin, this prevented the infection induced increase in mRNA levels of GlyP, the limiting enzyme for glycogen mobilization (Figure 7C). Moreover, we saw that infection-mediated mobilization of glycogen was reduced in rapamycin-fed animals (Figure 7D). Taken together, these results suggest that infection leads to depletion of stored glycogen in part through TOR signaling. Thus, one possibility is that this TOR-dependent mobilization of glycogen is used to fuel tissue metabolism during infection and also may provide glucose for TOR-induced de novo synthesis of TAGs.

DISCUSSION

In this paper we show that enteric infection with Gram-negative bacteria leads to both a local (intestinal) and systemic increase in TOR signaling. We found that this induction is required to replenish mobilized lipid stores and is needed for optimal survival following infection. We found that the induction of TOR occurred independently of either IMD or ROS signaling, the two best-studied pathways induced upon enteric infection with Gram-negative bacteria, Instead, our data suggest that enteric infection induces a direct stimulation of TOR in the intestine and also a non-autonomous induction of systemic insulin/PI3K signaling.

It is interesting to compare our results with previous work examining enteric infection and TOR signaling. One study showed that oral infection with the Gram-negative bacteria, *Ecc15,* induced a rapid induction of intestinal TOR activity, as measured by phosphorylation of the TOR effector 4EBP, and that this induction was specifically seen in the intestinal stem cells (Haller *et al.*, 2017). We saw a similar induction of TOR in stem cell, but we observed that it also occurred in the large enterocytes, the main absorptive, barrier and metabolic cells of the intestine. In contrast to both this study and our work, another paper showed that *P.e.* infection actually led to a reduction in TOR and a decrease in protein synthesis (Chakrabarti *et al.*, 2012). We found that the induction of TOR signaling was accompanied by an increase in levels of tRNAs, pre-RNA and ribosome synthesis genes, each of which are known to be targets of TOR signaling (Grewal et al., 2007; Li et al., 2010; Marshall *et al.*, 2012), suggesting an increase in protein synthesis. The reasons for each of these differences in TOR responses to enteric infection could be due to differences in either the pathogenicity or levels of the enteric bacteria. Alternatively, they may reflect differences in fly diet and/or commensal bacterial between each study. Indeed, cross-talk between commensal and

Disease Models & Mechanisms • DMM • Accepted manuscript

pathogenic bacteria as well as interactions with dietary nutrients have been shown to impact intestinal physiology and gut epithelial responses (McCarville et al., 2020). These effects are often mediated through bacterial-derived small molecules or metabolites. Given that intracellular TOR signaling can be stimulated by extracellular small molecules such as amino acids, nucleotides, and sugars (Ben-Sahra and Manning, 2017; Valvezan and Manning, 2019), it is possible that these mechanisms may explain the induction of intestinal TOR that we observed.

Our data suggest that the systemic induction of TOR may rely on insulin/PI3K signaling. Thus, we saw that enteric infection increased Akt phosphorylation and altered expression of FOXO targets in whole animals and remote tissues such as the abdominal fat tissues. The insulin pathway is one of the main endocrine regulators of metabolism in flies and extensive work has shown that one main way that it is stimulated is through increased expression of brain-derived dILPs in response to peripheral tissue-to-brain signaling (Grewal, 2012; Koyama *et al.*, 2020). We saw increased expression of three dilps, suggesting a potential role for gut-to-brain signaling. Indeed, some of the gut-derived peptides in flies have previously been shown to control brain dILP expression (Alfa et al., 2015; Ren et al., 2015; Sano et al., 2015; Yoshinari et al., 2021) and infection has been shown to stimulate the enteroendocrine cells that produce these peptides (Park et al., 2016). Interestingly, our induction of systemic insulin with *P.e.* contrasts with studies showing other bacterial pathogens such as *V. cholerae* and *M. Marinum* can suppress insulin/PI3K signaling in flies (Dionne *et al.*, 2006; Hang et al., 2014), suggesting that the type of pathogenic bacteria is an important determinant of host physiological responses.

We found that the stimulation of TOR signaling by *P.e.* infection was not required for induction of the AMPs, the main anti-bacterial resistance response in flies, and had no effect on pathogen burden. The AMPs are primarily induced by IMD/Relish signalling following enteric infection. Interestingly we saw that infection survival was reduced only when we simultaneously blocked both IMD signaling (*relish* mutants) and TOR signaling (rapamycin feeding). Based on these data, one simple model is that upon infection, the IMD pathway is induced to initiate resistance (antibacterial defences), while TOR induction plays a role in tolerance responses (adaption to pathogen infection). Another possibility, is that the effects of TOR induction become important when the IMD pathway is comprised, hence leading to exacerbated death in *relish* mutants treated with rapamycin.

Disease Models & Mechanisms • DMM • Accepted manuscript

Tolerance responses are defined as alterations in host biology that limit pathology and promote survival without affecting pathogen load (Ayres and Schneider, 2012; Medzhitov *et al.*, 2012). These can involve adaptations in host metabolism (Cumnock et al., 2018), changes in host behaviour, or induction of host tissue protective and repair processes (Martins et al., 2019). It is becoming clear that these responses are as important as resistance (anti-pathogenic) responses in determining host survival upon infection, and, as a result, there is increasing interest in determining mechanisms that control tolerance. In the context of enteric infection, recent studies have emphasized how gut-mediated changes in whole-body level physiological programs such as systemic insulin signaling and glucose and lipid metabolism play an important role in tolerance responses (Sanchez *et al.*, 2018; Schieber et al., 2015). We saw that enteric infection led to a transient reduction in total TAGs and a decrease in intestinal and fat body lipid stores. These results are consistent with previous reports that also described how both enteric and systemic infection with pathogenic bacteria such as *M. Marinum,* and *V. cholera* can reduce both intestinal and fat body lipid levels (Dionne *et al.*, 2006; Hang *et al.*, 2014; Kamareddine *et al.*, 2018a; Kamareddine et al., 2018b; Zhao and Karpac, 2021). Constitutive activation of the IMD pathway in the *Drosophila* fat body can promote lipid mobilization (Davoodi et al., 2019), suggesting that lipid loss may be a general feature of infection with pathogenic bacteria in flies. One likely possibility is that this lipid loss reflects mobilization of lipid stores to fuel energetically costly host immune responses perhaps through a switch to fatty acid oxidation which is often a type of metabolic reprogramming seen upon infection (Cumnock *et al.*, 2018). We saw that infection increased the expression of lipoproteins that are needed for transport of fat body- and gut-derived lipids to other tissues. Moreover, a recent study described inter-individual differences in mobilization and transport of lipids via these lipoproteins is a key determinant of infection susceptibility (Zhao and Karpac, 2021).

In the context of infection-mediated lipid mobilization, we saw that one function for TOR appeared to be limit excess lipid loss. Thus, when we rapamycin-treated flies we saw that the transient decrease in lipid stores following infection developed into a progressive loss of lipid stores. Our results suggest that TOR functions to prevent excess lipid loss by promoting de novo lipid synthesis through increased expression of lipid synthesis genes and two transcription factors, Mondo and SREBP, that control the expression of these genes (Heier and Kuhnlein, 2018; Mattila and Hietakangas, 2017). These lipid synthesis genes are enriched for expression in the fat body, oenocyte and the intestine (Leader et al., 2018) and we saw increased expression in both intestinal

Disease Models & Mechanisms • DMM • Accepted manuscript

and isolated abdominal samples (that are enriched in fat body and oenocytes). We therefore propose that enteric pathogens can, through direct effects on the gut and indirect effects on systemic insulin, increase TOR activity in the gut and the abdominal adipose tissues (fat body/oenocytes) to stimulate lipid synthesis gene expression in these organs. It is also possible that TOR regulation of lipid metabolism in one tissue may non-autonomously mediate effects on lipid metabolism in other tissues as has been described (Kamareddine *et al.*, 2018a; Song et al., 2014; Zhao and Karpac, 2017; 2020). Future studies using tissue-specific genetic modulation may help pin-point each of the specific sites(s) of TOR action. We also found that TOR signaling regulated glycogen mobilization following infection: we saw that rapamycin blocked the induction of glycogen phosphate, which is required to mobilize glycogen, and we saw that the infection-mediated loss of glycogen was partially prevented by rapamycin. Together, our data suggest that upon infection, TOR is required to limit lipid loss but is needed for proper glycogen mobilization, which may be used to fuel immune metabolic responses, and perhaps also to supply the glucose needed for de novo lipid synthesis.

A central theme of our work is that alterations in host lipid metabolism are important component of immune responses. This is supported by previous studies in flies that have described how both intestinal and fat body lipid metabolism are needed for effective immune responses (Chakrabarti et al., 2014; Harsh et al., 2019; Kamareddine *et al.*, 2018a; Lee *et al.*, 2018; Martinez et al., 2020). Our work pinpoints TOR as a central modulator of enteric infection-mediated changes in lipid metabolism, likely as a mechanism of infection tolerance. The intestine also plays a central role coordinating other aspects of fly physiology such as repair of local tissue damage (Colombani and Andersen, 2020) and modulation of feeding behavior (Hadjieconomou et al., 2020; Miguel-Aliaga *et al.*, 2018; Redhai et al., 2020). Given previous work implicating these processes as regulators of infection tolerance (Ayres and Schneider, 2012; Rao et al., 2017), our finding that TOR is induced in the gut suggest it may also play a role in these other important responses to infection.

METHODS

Drosophila stocks and culturing

Flies were kept on medium containing 150 g agar, 1600 g cornmeal, 770 g Torula yeast, 675 g sucrose, 2340 g D-glucose, 240 ml acid mixture (propionic acid/phosphoric acid) per 34 L water and maintained at 25°C. The following lines were used in this study (Blooington stock numbers

Disease Models & Mechanisms • DMM • Accepted manuscript

indicated) : w^{1118}, $imd^{[EY08573]}$ (17474), $rel^{E20]}$ (9457) , $rel^{E38]}$ (9458), *UAS-ImpL2* (Sarraf-Zadeh et al., 2013), *da-geneswitch-Gal4* (Sun et al., 2014). Induction of gene expression using the *GeneSwitch* system was done by feeding flies RU486 (100μM) for 3 days.

Enteric Infections

Enteric infections were performed using previously described methods (Buchon et al., 2010; Zhao and Karpac, 2021). Briefly, *Pseudomonas entomophila* (*P.e*) from overnight cultures were pelleted and resuspended in 5% sucrose solution (in sterile water) such that the final concentration of bacteria was OD_{600}= 200, except for the experiment described in Figure S4C where concentrations from OD_{600}= 1-200 were tested. To prepare infection vials, bacterial pellets were dissolved in filter sterilized 5% sucrose/PBS. Chromatography paper (Fisher, Pittsburgh, PA) discs were dipped in the bacterial solution (5% sucrose was used as a control) and were carefully placed on standard fly food vials such that they covered the entire food surface. Adult females were first subjected to a 2-hr starvation in empty vials at 29°C. Then 10-12 flies were transferred to each infection vial and then placed in a 29°C incubator for the duration of the assay.

Adult survival assay

Adult female flies were infected as above. Post infection the flies were transferred to fresh food vials every 2 days. The number of deaths was scored every 24hrs.

Rapamycin and chemical feeding:

For treatment with rapamycin, 3-5 day old female flies were shifted on vials containing 100μM rapamycin dissolved in standard *Drosophila* food for 24hrs. DMSO dissolved in food was used as a control. After 24hr of rapamycin pre-treatment, the flies were then transferred to infection vials mixed with 100μM final concentration of rapamycin or DMSO. Chemical intestine stressors, [25μg/ml Bleomycin (Sigma # 9041-93-4), 5%DSS (Sigma, #9011-18-1) 2mM paraquat (Sigma, #75365-73-0)] were used to induce intestine specific stress in w^{1118} flies. To block ROS, flies were fed the antioxidant, N-acetyl cysteine at a concentration of 100mM. Uracil was fed at a concentration of 20 nM. 5% sucrose solution was used as a solvent for all the mentioned chemicals. 5% Sucrose solution alone was used as the control for all experiments. 500μl of each solution was used to completely soak a piece of 2.5 cm × 3.75 cm chromatography paper (Fisher, Pittsburgh, PA), which was then placed inside an empty vial). 5–7-day old, mated females (n=10-12/ vial) were then added to the vials.

Disease Models & Mechanisms • DMM • Accepted manuscript

Bacterial Load measurements:

Adult flies were surface sterilized by washing in 70% ethanol and then sterile PBS. Groups of five flies were then homogenized using a sterile pestle. The homogenate was then serially diluted, and the serial dilutions were plated onto LB plates and incubated overnight at 29C. The number of separate, well-defined colonies on each plate were then counted. The number of colony forming units (CFU)/fly for each plate was calculated using the following formula:
CFU/fly = [(colony number)*(dilution factor)/plating volume]*total volume of initial homogenate/5 (number of flies per condition).

SDS-PAGE and western Blotting

Intestines (10 per sample) were dissected in ice cold 1X PBS and immediately lysed in ice cold lysis buffer containing 20 mM Tris-HCl (pH 8.0), 137 mM NaCl, 1 mM EDTA, 25 % glycerol, 1% NP-40, 50 mM NaF, 1 mM PMSF, 1 mM DTT, 5 mM sodium ortho vanadate (Na_3VO_4) and Protease Inhibitor cocktail (Roche Cat. No. 04693124001) and Phosphatase inhibitor (Roche Cat. No. 04906845001). Protein concentrations were measured using the Bio-Rad Dc Protein Assay kit II (5000112). Protein lysates (15 μg to 30μg) were resolved by SDS–PAGE and transferred to a nitrocellulose membrane, and then subjected to western blotting with specific primary antibodies and HRP-conjugated secondary antibodies, and then visualized by chemiluminescence (enhanced ECL solution (Perkin Elmer). Primary antibodies used in this study were: anti-phospho-S6K-Thr398 (1:1000, Cell Signalling Technology #9209), anti-pERK T980 (Cell signaling technology #3179, 1:1000 dilution), anti-pAkt-S505 (Cell Signaling #4054, 1:1000 dilution), anti-phospho S6 (1:500, gift from Aurelio Teleman) and anti-actin (1:1000, Santa Cruz Biotechnology, # sc-8432). Secondary antibodies were purchased from Santa Cruz Biotechnology (sc-2030, 2005, 2020, 1:10,000 dilution). Blots and band intensities were quantified using Image-J.

Phospho S6 Immunostaining

Intestines were dissected in ice cold 1X PBS and then fixed in 4% Paraformaldehyde in 1X PBS (1:4 diluted from Pierce™ 16% Formaldehyde Cat # 28906) at room temperature for 30 mins. Post fixation, the tissues were washed with 1X PBS + 0.1% TritonX100, for 10 mins. The tissues were then blocked in 1X PAT buffer + 2% fetal bovine serum (FBS) for 2hrs at RT. The tissues were then transferred to fresh PAT containing the primary antibody, overnight at 4°C. The primary antibody (anti-phospho S6, 1:200) incubation was followed by 3 washes at RT with 1X PBT + 2% fetal bovine serum (FBS) for 30 mins each. The tissues were then incubated with secondary antibody in PBT

Disease Models & Mechanisms • DMM • Accepted manuscript

without the serum at RT for 2 hours, followed by 3 x 30 min washes in PBT without serum at RT. Finally, the tissues were incubated with 1:10000 of Hoechst 33342 (Invitrogen) in PBT to stain the nuclei. The tissues were then mounted on glass slides with coverslips, using Vectashield (Vector laboratories Inc., CA). The slides were visualized under a Zeiss Observer Z1 microscope using the 10x and 20x objectives and with Zen- Axiovision software. When analyzing and capturing images, exposure levels were kept constant across all conditions and samples analyzed. At least 10 independent tissue samples were profiled in each experiment and representative images are shown in the Figures.

Quantitative Real Time Polymerase Chain Reaction (qRT-PCR):

Total RNA was extracted from groups of 5 adults or 10 intestines using TRIzol reagent according to manufacturer's instructions (Invitrogen; 15596–018). The RNA samples were treated with DNase (Ambion; 2238 G) and then reverse transcribed using Superscript II (Invitrogen; 100004925). The cDNAs were then used as a template for subsequent qRT–PCRs using SyBr Green PCR mix (Thermofisher) and an ABI 7500 real time PCR system. The PCR data were normalized to actin mRNA or 5S RNA levels. The primers used in this study can be found in Supplemental Table 1.

Bodipy staining

The adult intestines were dissected in ice cold 1X PBS. The tissue samples were then fixed in 4% Paraformaldehyde in 1X PBS (1:4 diluted from Pierce™ 16% Formaldehyde Cat # 28906) at room temperature for 30 mins. The fixation was followed by a couple washes for 5 minutes at RT with PBS. The BODIPY (Invitrogen) was diluted in PBS (1:100) for 30mins at RT. The samples were then washed twice with PBS for 10min. Finally, the tissues were incubated with 1:10000dil of Hoechst 33342 (Invitrogen) in PBT to stain the nuclei, followed by another wash with PBS for 10mins at RT. The tissues were then mounted on slides and visualized as mentioned above. At least 10 independent samples were profiled for each condition. Representative images were shown in the figures.

Oil Red O staining

The adult intestines were dissected in ice cold PBS. The tissue samples were then fixed in 4% paraformaldehyde in PBS at RT for 30 mins. The fixation was followed by a couple washes for 5 min at RT with PBS. The intestines were then incubated in fresh Oil Red O (Sigma- Aldrich Cat # O0625) solution. The solution was prepared by adding 6ml of 0.1% Oil Red O in Isopropanol and 4ml ultra-

Disease Models & Mechanisms • DMM • Accepted manuscript

pure dH_2O, passed through 0.45µm syringe), followed by rinsing with distilled water. The tissues were mounted on a glass slide and the tissues were imaged using a dissecting microscope. At least 10 independent samples were profiled for each condition. Representative images were shown in the figures.

TAG and glycogen assays

The metabolic assays were performed as previously described (Tennessen et al., 2014). Briefly, animals were lysed, and lysates were heated at 70 Celsius for 10 minutes. Then they were incubated first with triglyceride reagent (Sigma; T2449) and then mixed with free glycerol reagent (Sigma; F6428). Colorimetric measurements were then made using absorbance at 540 nm and TAG levels calculated by comparing with a glycerol standard curve. Glycogen assays were performed by lysing animals in PBS and then heating lysates at 70 Celsius for 10 minutes. For each experimental sample, duplicate samples were either treated with amyloglucosidase (Sigma A1602) to breakdown glycogen intro glucose, or left untreated, and then levels of glucose in both duplicates measured by colorimetric assay following the addition of a glucose oxidase reagent (Sigma; GAGO-20). Levels of glycogen in each experimental sample were then calculated by subtracting the glucose measurements of the untreated duplicate from the amyloglucosidase-treated sample. All experimental metabolite concentrations were calculated by comparison with glycogen and glucose standard curves.

ACKNOWLEDGEMENTS

We thank Edan Foley, Sige Zou and Nicholas Buchon for the gift of fly and bacterial stocks. Stocks obtained from the Bloomington *Drosophila* Stock Center (NIH P40OD018537) were used in this study. This work was supported by a CIHR project grant and NSERC discovery grant to S.S.G.

Disease Models & Mechanisms • DMM • Accepted manuscript

REFERENCES

Alfa, R.W., Park, S., Skelly, K.R., Poffenberger, G., Jain, N., Gu, X., Kockel, L., Wang, J., Liu, Y., Powers, A.C., and Kim, S.K. (2015). Suppression of insulin production and secretion by a decretin hormone. Cell metabolism *21*, 323-334. 10.1016/j.cmet.2015.01.006.

Allen, V.W., O'Connor, R.M., Ulgherait, M., Zhou, C.G., Stone, E.F., Hill, V.M., Murphy, K.R., Canman, J.C., Ja, W.W., and Shirasu-Hiza, M.M. (2016). period-Regulated Feeding Behavior and TOR Signaling Modulate Survival of Infection. Current biology : CB *26*, 184-194. 10.1016/j.cub.2015.11.051.

Ayres, J.S., and Schneider, D.S. (2012). Tolerance of infections. Annu Rev Immunol *30*, 271-294. 10.1146/annurev-immunol-020711-075030.

Ben-Sahra, I., and Manning, B.D. (2017). mTORC1 signaling and the metabolic control of cell growth. Current opinion in cell biology *45*, 72-82. 10.1016/j.ceb.2017.02.012.

Boulan, L., Milan, M., and Leopold, P. (2015). The Systemic Control of Growth. Cold Spring Harb Perspect Biol *7*. 10.1101/cshperspect.a019117.

Buchon, N., Broderick, N.A., Kuraishi, T., and Lemaitre, B. (2010). Drosophila EGFR pathway coordinates stem cell proliferation and gut remodeling following infection. BMC Biol *8*, 152. 10.1186/1741-7007-8-152.

Buchon, N., Silverman, N., and Cherry, S. (2014). Immunity in Drosophila melanogaster--from microbial recognition to whole-organism physiology. Nat Rev Immunol *14*, 796-810. 10.1038/nri3763.

Chakrabarti, S., Liehl, P., Buchon, N., and Lemaitre, B. (2012). Infection-induced host translational blockage inhibits immune responses and epithelial renewal in the Drosophila gut. Cell Host Microbe *12*, 60-70. 10.1016/j.chom.2012.06.001.

Chakrabarti, S., Poidevin, M., and Lemaitre, B. (2014). The Drosophila MAPK p38c regulates oxidative stress and lipid homeostasis in the intestine. PLoS genetics *10*, e1004659. 10.1371/journal.pgen.1004659.

Disease Models & Mechanisms • DMM • Accepted manuscript

Chambers, M.C., Song, K.H., and Schneider, D.S. (2012). Listeria monocytogenes infection causes metabolic shifts in Drosophila melanogaster. PLoS One *7*, e50679. 10.1371/journal.pone.0050679.

Colombani, J., and Andersen, D.S. (2020). The Drosophila gut: A gatekeeper and coordinator of organism fitness and physiology. Wiley Interdiscip Rev Dev Biol *9*, e378. 10.1002/wdev.378.

Cumnock, K., Gupta, A.S., Lissner, M., Chevee, V., Davis, N.M., and Schneider, D.S. (2018). Host Energy Source Is Important for Disease Tolerance to Malaria. Current biology : CB *28*, 1635-1642 e1633. 10.1016/j.cub.2018.04.009.

Davoodi, S., Galenza, A., Panteluk, A., Deshpande, R., Ferguson, M., Grewal, S., and Foley, E. (2019). The Immune Deficiency Pathway Regulates Metabolic Homeostasis in Drosophila. J Immunol *202*, 2747-2759. 10.4049/jimmunol.1801632.

Dionne, M.S., Pham, L.N., Shirasu-Hiza, M., and Schneider, D.S. (2006). Akt and FOXO dysregulation contribute to infection-induced wasting in Drosophila. Current biology : CB *16*, 1977-1985. 10.1016/j.cub.2006.08.052.

Galenza, A., and Foley, E. (2019). Immunometabolism: Insights from the Drosophila model. Dev Comp Immunol *94*, 22-34. 10.1016/j.dci.2019.01.011.

Ganeshan, K., Nikkanen, J., Man, K., Leong, Y.A., Sogawa, Y., Maschek, J.A., Van Ry, T., Chagwedera, D.N., Cox, J.E., and Chawla, A. (2019). Energetic Trade-Offs and Hypometabolic States Promote Disease Tolerance. Cell *177*, 399-413 e312. 10.1016/j.cell.2019.01.050.

Ghosh, A., Rideout, E.J., and Grewal, S.S. (2014). TIF-IA-dependent regulation of ribosome synthesis in drosophila muscle is required to maintain systemic insulin signaling and larval growth. PLoS genetics *10*, e1004750. 10.1371/journal.pgen.1004750.

Grewal, S.S. (2009). Insulin/TOR signaling in growth and homeostasis: a view from the fly world. Int J Biochem Cell Biol *41*, 1006-1010. 10.1016/j.biocel.2008.10.010.

Grewal, S.S. (2012). Controlling animal growth and body size - does fruit fly physiology point the way? F1000 Biol Rep *4*, 12. 10.3410/B4-12.

Disease Models & Mechanisms • DMM • Accepted manuscript

Grewal, S.S., Evans, J.R., and Edgar, B.A. (2007). Drosophila TIF-IA is required for ribosome synthesis and cell growth and is regulated by the TOR pathway. J Cell Biol *179*, 1105-1113. 10.1083/jcb.200709044.

Hadjieconomou, D., King, G., Gaspar, P., Mineo, A., Blackie, L., Ameku, T., Studd, C., de Mendoza, A., Diao, F., White, B.H., et al. (2020). Enteric neurons increase maternal food intake during reproduction. Nature *587*, 455-459. 10.1038/s41586-020-2866-8.

Haller, S., Kapuria, S., Riley, R.R., O'Leary, M.N., Schreiber, K.H., Andersen, J.K., Melov, S., Que, J., Rando, T.A., Rock, J., et al. (2017). mTORC1 Activation during Repeated Regeneration Impairs Somatic Stem Cell Maintenance. Cell Stem Cell *21*, 806-818 e805. 10.1016/j.stem.2017.11.008.

Hang, S., Purdy, A.E., Robins, W.P., Wang, Z., Mandal, M., Chang, S., Mekalanos, J.J., and Watnick, P.I. (2014). The acetate switch of an intestinal pathogen disrupts host insulin signaling and lipid metabolism. Cell Host Microbe *16*, 592-604. 10.1016/j.chom.2014.10.006.

Harsh, S., Heryanto, C., and Eleftherianos, I. (2019). Intestinal lipid droplets as novel mediators of host-pathogen interaction in Drosophila. Biol Open *8*. 10.1242/bio.039040.

Heier, C., and Kuhnlein, R.P. (2018). Triacylglycerol Metabolism in Drosophila melanogaster. Genetics *210*, 1163-1184. 10.1534/genetics.118.301583.

Howell, J.J., Ricoult, S.J., Ben-Sahra, I., and Manning, B.D. (2013). A growing role for mTOR in promoting anabolic metabolism. Biochem Soc Trans *41*, 906-912. 10.1042/BST20130041.

Kamareddine, L., Robins, W.P., Berkey, C.D., Mekalanos, J.J., and Watnick, P.I. (2018a). The Drosophila Immune Deficiency Pathway Modulates Enteroendocrine Function and Host Metabolism. Cell metabolism *28*, 449-462 e445. 10.1016/j.cmet.2018.05.026.

Kamareddine, L., Wong, A.C.N., Vanhove, A.S., Hang, S., Purdy, A.E., Kierek-Pearson, K., Asara, J.M., Ali, A., Morris, J.G., Jr., and Watnick, P.I. (2018b). Activation of Vibrio cholerae quorum sensing promotes survival of an arthropod host. Nat Microbiol *3*, 243-252. 10.1038/s41564-017-0065-7.

Disease Models & Mechanisms • DMM • Accepted manuscript

Killip, L.E., and Grewal, S.S. (2012). DREF is required for cell and organismal growth in Drosophila and functions downstream of the nutrition/TOR pathway. Developmental biology *371*, 191-202. 10.1016/j.ydbio.2012.08.020.

Kleino, A., and Silverman, N. (2014). The Drosophila IMD pathway in the activation of the humoral immune response. Dev Comp Immunol *42*, 25-35. 10.1016/j.dci.2013.05.014.

Koyama, T., Texada, M.J., Halberg, K.A., and Rewitz, K. (2020). Metabolism and growth adaptation to environmental conditions in Drosophila. Cell Mol Life Sci *77*, 4523-4551. 10.1007/s00018-020-03547-2.

Krejcova, G., Danielova, A., Nedbalova, P., Kazek, M., Strych, L., Chawla, G., Tennessen, J.M., Lieskovska, J., Jindra, M., Dolezal, T., and Bajgar, A. (2019). Drosophila macrophages switch to aerobic glycolysis to mount effective antibacterial defense. eLife *8*. 10.7554/eLife.50414.

Leader, D.P., Krause, S.A., Pandit, A., Davies, S.A., and Dow, J.A.T. (2018). FlyAtlas 2: a new version of the Drosophila melanogaster expression atlas with RNA-Seq, miRNA-Seq and sex-specific data. Nucleic Acids Res *46*, D809-D815. 10.1093/nar/gkx976.

Lee, J.E., Rayyan, M., Liao, A., Edery, I., and Pletcher, S.D. (2017). Acute Dietary Restriction Acts via TOR, PP2A, and Myc Signaling to Boost Innate Immunity in Drosophila. Cell reports *20*, 479-490. 10.1016/j.celrep.2017.06.052.

Lee, K.A., Cho, K.C., Kim, B., Jang, I.H., Nam, K., Kwon, Y.E., Kim, M., Hyeon, D.Y., Hwang, D., Seol, J.H., and Lee, W.J. (2018). Inflammation-Modulated Metabolic Reprogramming Is Required for DUOX-Dependent Gut Immunity in Drosophila. Cell Host Microbe *23*, 338-352 e335. 10.1016/j.chom.2018.01.011.

Lee, K.A., Kim, B., Bhin, J., Kim, D.H., You, H., Kim, E.K., Kim, S.H., Ryu, J.H., Hwang, D., and Lee, W.J. (2015). Bacterial uracil modulates Drosophila DUOX-dependent gut immunity via Hedgehog-induced signaling endosomes. Cell Host Microbe *17*, 191-204. 10.1016/j.chom.2014.12.012.

Lee, K.A., and Lee, W.J. (2018). Immune-metabolic interactions during systemic and enteric infection in Drosophila. Curr Opin Insect Sci *29*, 21-26. 10.1016/j.cois.2018.05.014.

Disease Models & Mechanisms • DMM • Accepted manuscript

Li, L., Edgar, B.A., and Grewal, S.S. (2010). Nutritional control of gene expression in Drosophila larvae via TOR, Myc and a novel cis-regulatory element. BMC Cell Biol *11*, 7. 10.1186/1471-2121-11-7.

Luis, N.M., Wang, L., Ortega, M., Deng, H., Katewa, S.D., Li, P.W., Karpac, J., Jasper, H., and Kapahi, P. (2016). Intestinal IRE1 Is Required for Increased Triglyceride Metabolism and Longer Lifespan under Dietary Restriction. Cell reports *17*, 1207-1216. 10.1016/j.celrep.2016.10.003.

Man, K., Kutyavin, V.I., and Chawla, A. (2017). Tissue Immunometabolism: Development, Physiology, and Pathobiology. Cell metabolism *25*, 11-26. 10.1016/j.cmet.2016.08.016.

Marshall, L., Rideout, E.J., and Grewal, S.S. (2012). Nutrient/TOR-dependent regulation of RNA polymerase III controls tissue and organismal growth in Drosophila. EMBO J *31*, 1916-1930. 10.1038/emboj.2012.33.

Martinez, B.A., Hoyle, R.G., Yeudall, S., Granade, M.E., Harris, T.E., Castle, J.D., Leitinger, N., and Bland, M.L. (2020). Innate immune signaling in Drosophila shifts anabolic lipid metabolism from triglyceride storage to phospholipid synthesis to support immune function. PLoS genetics *16*, e1009192. 10.1371/journal.pgen.1009192.

Martins, R., Carlos, A.R., Braza, F., Thompson, J.A., Bastos-Amador, P., Ramos, S., and Soares, M.P. (2019). Disease Tolerance as an Inherent Component of Immunity. Annu Rev Immunol *37*, 405-437. 10.1146/annurev-immunol-042718-041739.

Mattila, J., and Hietakangas, V. (2017). Regulation of Carbohydrate Energy Metabolism in Drosophila melanogaster. Genetics *207*, 1231-1253. 10.1534/genetics.117.199885.

Mayer, C., and Grummt, I. (2006). Ribosome biogenesis and cell growth: mTOR coordinates transcription by all three classes of nuclear RNA polymerases. Oncogene *25*, 6384-6391.

McCarville, J.L., Chen, G.Y., Cuevas, V.D., Troha, K., and Ayres, J.S. (2020). Microbiota Metabolites in Health and Disease. Annu Rev Immunol *38*, 147-170. 10.1146/annurev-immunol-071219-125715.

Disease Models & Mechanisms • DMM • Accepted manuscript

Medzhitov, R., Schneider, D.S., and Soares, M.P. (2012). Disease tolerance as a defense strategy. Science (New York, N.Y.) *335*, 936-941. 10.1126/science.1214935.

Miguel-Aliaga, I., Jasper, H., and Lemaitre, B. (2018). Anatomy and Physiology of the Digestive Tract of Drosophila melanogaster. Genetics *210*, 357-396. 10.1534/genetics.118.300224.

Park, J.H., Chen, J., Jang, S., Ahn, T.J., Kang, K., Choi, M.S., and Kwon, J.Y. (2016). A subset of enteroendocrine cells is activated by amino acids in the Drosophila midgut. FEBS Lett *590*, 493-500. 10.1002/1873-3468.12073.

Rao, S., Schieber, A.M.P., O'Connor, C.P., Leblanc, M., Michel, D., and Ayres, J.S. (2017). Pathogen-Mediated Inhibition of Anorexia Promotes Host Survival and Transmission. Cell *168*, 503-516 e512. 10.1016/j.cell.2017.01.006.

Redhai, S., Pilgrim, C., Gaspar, P., Giesen, L.V., Lopes, T., Riabinina, O., Grenier, T., Milona, A., Chanana, B., Swadling, J.B., et al. (2020). An intestinal zinc sensor regulates food intake and developmental growth. Nature *580*, 263-268. 10.1038/s41586-020-2111-5.

Ren, G.R., Hauser, F., Rewitz, K.F., Kondo, S., Engelbrecht, A.F., Didriksen, A.K., Schjott, S.R., Sembach, F.E., Li, S., Sogaard, K.C., et al. (2015). CCHamide-2 Is an Orexigenic Brain-Gut Peptide in Drosophila. PLoS One *10*, e0133017. 10.1371/journal.pone.0133017.

Rideout, E.J., Marshall, L., and Grewal, S.S. (2012). Drosophila RNA polymerase III repressor Maf1 controls body size and developmental timing by modulating tRNAiMet synthesis and systemic insulin signaling. Proc Natl Acad Sci U S A *109*, 1139-1144. 10.1073/pnas.1113311109.

Sanchez, K.K., Chen, G.Y., Schieber, A.M.P., Redford, S.E., Shokhirev, M.N., Leblanc, M., Lee, Y.M., and Ayres, J.S. (2018). Cooperative Metabolic Adaptations in the Host Can Favor Asymptomatic Infection and Select for Attenuated Virulence in an Enteric Pathogen. Cell *175*, 146-158 e115. 10.1016/j.cell.2018.07.016.

Disease Models & Mechanisms • DMM • Accepted manuscript

Sano, H., Nakamura, A., Texada, M.J., Truman, J.W., Ishimoto, H., Kamikouchi, A., Nibu, Y., Kume, K., Ida, T., and Kojima, M. (2015). The Nutrient-Responsive Hormone CCHamide-2 Controls Growth by Regulating Insulin-like Peptides in the Brain of Drosophila melanogaster. PLoS genetics *11*, e1005209. 10.1371/journal.pgen.1005209.

Sarraf-Zadeh, L., Christen, S., Sauer, U., Cognigni, P., Miguel-Aliaga, I., Stocker, H., Kohler, K., and Hafen, E. (2013). Local requirement of the Drosophila insulin binding protein imp-L2 in coordinating developmental progression with nutritional conditions. Developmental biology *381*, 97-106. 10.1016/j.ydbio.2013.06.008.

Saxton, R.A., and Sabatini, D.M. (2017). mTOR Signaling in Growth, Metabolism, and Disease. Cell *168*, 960-976. 10.1016/j.cell.2017.02.004.

Schieber, A.M., Lee, Y.M., Chang, M.W., Leblanc, M., Collins, B., Downes, M., Evans, R.M., and Ayres, J.S. (2015). Disease tolerance mediated by microbiome E. coli involves inflammasome and IGF-1 signaling. Science (New York, N.Y.) *350*, 558-563. 10.1126/science.aac6468.

Schneider, D.S., and Ayres, J.S. (2008). Two ways to survive infection: what resistance and tolerance can teach us about treating infectious diseases. Nat Rev Immunol *8*, 889-895. 10.1038/nri2432.

Song, W., Veenstra, J.A., and Perrimon, N. (2014). Control of lipid metabolism by tachykinin in Drosophila. Cell reports *9*, 40-47. 10.1016/j.celrep.2014.08.060.

Sun, X., Wheeler, C.T., Yolitz, J., Laslo, M., Alberico, T., Sun, Y., Song, Q., and Zou, S. (2014). A mitochondrial ATP synthase subunit interacts with TOR signaling to modulate protein homeostasis and lifespan in Drosophila. Cell reports *8*, 1781-1792. 10.1016/j.celrep.2014.08.022.

Tennessen, J.M., Barry, W.E., Cox, J., and Thummel, C.S. (2014). Methods for studying metabolism in Drosophila. Methods *68*, 105-115. 10.1016/j.ymeth.2014.02.034.

Texada, M.J., Koyama, T., and Rewitz, K. (2020). Regulation of Body Size and Growth Control. Genetics *216*, 269-313. 10.1534/genetics.120.303095.

Disease Models & Mechanisms • DMM • Accepted manuscript

Troha, K., and Ayres, J.S. (2020). Metabolic Adaptations to Infections at the Organismal Level. Trends Immunol *41*, 113-125. 10.1016/j.it.2019.12.001.

Valvezan, A.J., and Manning, B.D. (2019). Molecular logic of mTORC1 signalling as a metabolic rheostat. Nat Metab *1*, 321-333. 10.1038/s42255-019-0038-7.

Varma, D., Bulow, M.H., Pesch, Y.Y., Loch, G., and Hoch, M. (2014). Forkhead, a new cross regulator of metabolism and innate immunity downstream of TOR in Drosophila. J Insect Physiol *69*, 80-88. 10.1016/j.jinsphys.2014.04.006.

Wang, A., Huen, S.C., Luan, H.H., Baker, K., Rinder, H., Booth, C.J., and Medzhitov, R. (2018). Glucose metabolism mediates disease tolerance in cerebral malaria. Proc Natl Acad Sci U S A *115*, 11042-11047. 10.1073/pnas.1806376115.

Wang, A., Huen, S.C., Luan, H.H., Yu, S., Zhang, C., Gallezot, J.D., Booth, C.J., and Medzhitov, R. (2016). Opposing Effects of Fasting Metabolism on Tissue Tolerance in Bacterial and Viral Inflammation. Cell *166*, 1512-1525 e1512. 10.1016/j.cell.2016.07.026.

Weis, S., Carlos, A.R., Moita, M.R., Singh, S., Blankenhaus, B., Cardoso, S., Larsen, R., Rebelo, S., Schauble, S., Del Barrio, L., et al. (2017). Metabolic Adaptation Establishes Disease Tolerance to Sepsis. Cell *169*, 1263-1275 e1214. 10.1016/j.cell.2017.05.031.

Wong, A.C., Vanhove, A.S., and Watnick, P.I. (2016). The interplay between intestinal bacteria and host metabolism in health and disease: lessons from Drosophila melanogaster. Dis Model Mech *9*, 271-281. 10.1242/dmm.023408.

Wu, S.C., Liao, C.W., Pan, R.L., and Juang, J.L. (2012). Infection-induced intestinal oxidative stress triggers organ-to-organ immunological communication in Drosophila. Cell Host Microbe *11*, 410-417. 10.1016/j.chom.2012.03.004.

Yang, S., Zhao, Y., Yu, J., Fan, Z., Gong, S.T., Tang, H., and Pan, L. (2019). Sugar Alcohols of Polyol Pathway Serve as Alarmins to Mediate Local-Systemic Innate Immune Communication in Drosophila. Cell Host Microbe *26*, 240-251 e248. 10.1016/j.chom.2019.07.001.

Disease Models & Mechanisms • DMM • Accepted manuscript

Yoshinari, Y., Kosakamoto, H., Kamiyama, T., Hoshino, R., Matsuoka, R., Kondo, S., Tanimoto, H., Nakamura, A., Obata, F., and Niwa, R. (2021). The sugar-responsive enteroendocrine neuropeptide F regulates lipid metabolism through glucagon-like and insulin-like hormones in Drosophila melanogaster. Nat Commun *12*, 4818. 10.1038/s41467-021-25146-w.

Zhao, X., and Karpac, J. (2017). Muscle Directs Diurnal Energy Homeostasis through a Myokine-Dependent Hormone Module in Drosophila. Current biology : CB *27*, 1941-1955 e1946. 10.1016/j.cub.2017.06.004.

Zhao, X., and Karpac, J. (2020). The Drosophila midgut and the systemic coordination of lipid-dependent energy homeostasis. Curr Opin Insect Sci *41*, 100-105. 10.1016/j.cois.2020.07.003.

Zhao, X., and Karpac, J. (2021). Glutamate metabolism directs energetic trade-offs to shape host-pathogen susceptibility in Drosophila. Cell metabolism *33*, 2428-2444 e2428. 10.1016/j.cmet.2021.10.003.

Disease Models & Mechanisms • DMM • Accepted manuscript

Figures

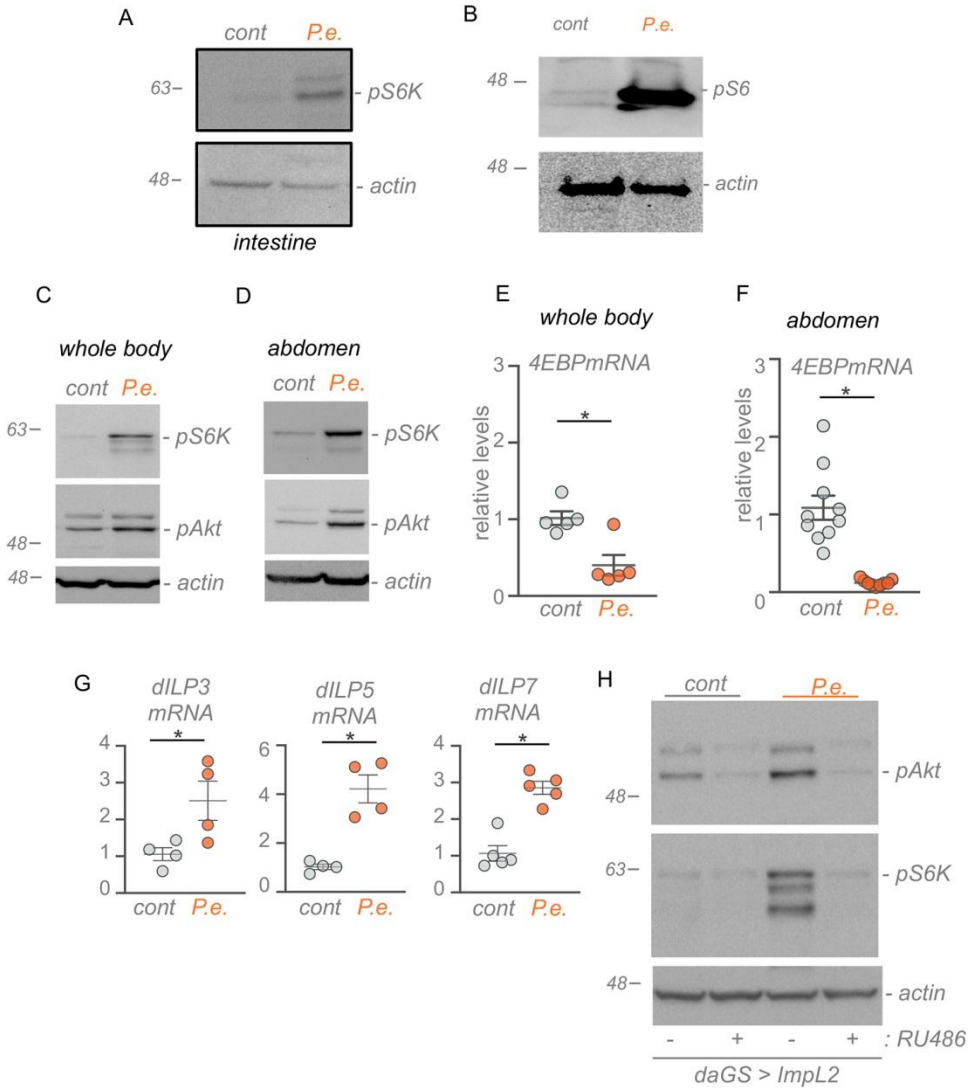

Figure 1. Enteric bacterial infection stimulates local and systemic TOR activity. A, B) Western blots of intestines from adult flies subjected to 4hr oral *P.e* infection using antibodies to A) phosphorylated S6K (pS6K), B) phosphorylated S6, and actin (as a loading control). C, D) Western blots of either C) whole animals or D) isolated abdominal samples from adult flies subjected to 4hr oral *P.e* infection using antibodies to phosphorylated S6K (pS6K), phosphorylated Akt, (pAkt) and actin (as a loading control) E, F) qPCR analysis of the FOXO target gene, 4EBP, from either E) whole-body samples, or F) abdominal samples of control or *P.e.* infected flies. Bars represent mean +/- SEM, individual data points are plotted as circles. *p<0.05, Students t-test. G). qPCR analysis of dILP

Disease Models & Mechanisms • DMM • Accepted manuscript

mRNAs from whole-body samples of control or *P.e.* infected flies. v H) Western blots of whole-body samples from control vs *P.e* infected adult flies (genotype: *daGAl4 GeneSwitch/+; UAS-ImpL2/+*) using antibodies to phosphorylated S6K (pS6K), phosphorylated Akt, (pAkt) and actin (as a loading control). ImpL2 induction was achieved by feeding flies RU486 for 3d prior to infection (+ RU486).

Disease Models & Mechanisms • DMM • Accepted manuscript

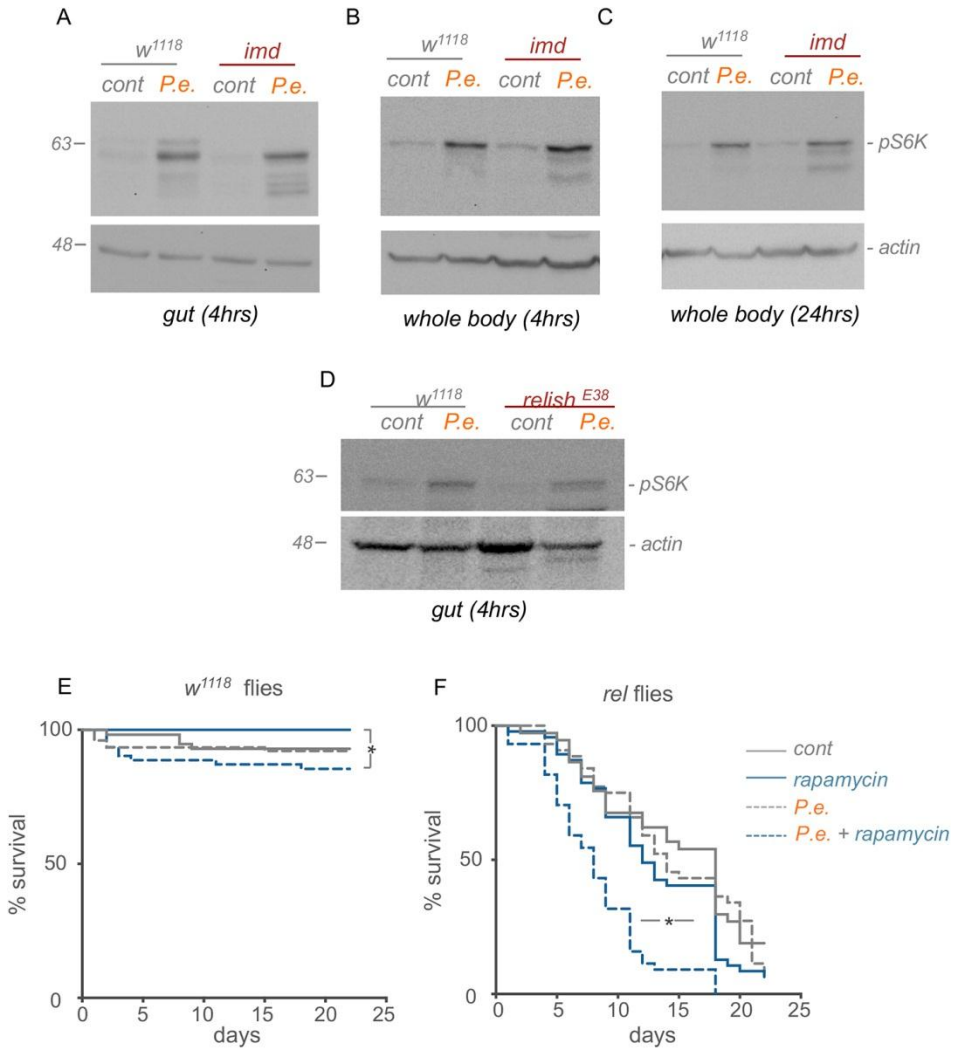

Figure 2. TOR and IMD signaling function in parallel to control survival in response to enteric infection. A-C) Western blots of A) intestinal, or B, C) whole-body samples from control vs *P.e* infected adult w^{1118} or immune deficiency (*imd*) mutants using antibodies to phosphorylated S6K and actin (as a loading control). D) Western blots of intestinal samples from control vs *P.e* infected adult w^{1118} or *relish* mutants using antibodies to phosphorylated S6K and actin (as a loading control). E) Survival plot of control w^{1118} (E) and $relish^{E20}$ (*rel*) mutant (F) mated female flies subjected to 48-hr oral *P.e.* infection. Animals were then returned to standard food and the percentage of animals surviving was counted. N = at least 50 animals per experimental condition. *p< 0.05, log rank test.

Disease Models & Mechanisms • DMM • Accepted manuscript

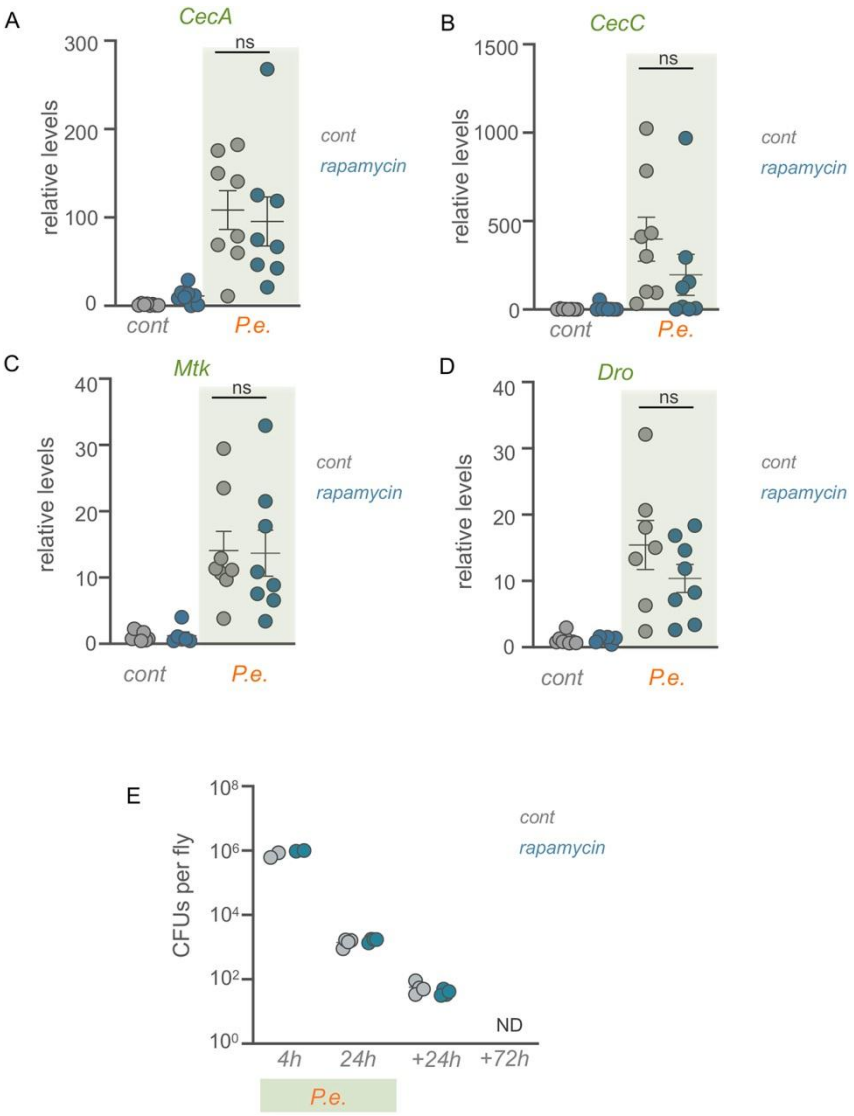

Figure 3. Induction of intestinal TOR signaling is not required for systemic AMP induction.
A) qRT- PCR analysis on adult w^{1118} mated females subjected to a 24hr pre-treatment of rapamycin or DMSO control followed by 24hr oral *P.e.* feeding along with rapamycin. mRNA transcript levels of anti-microbial peptides (AMPs) are presented as relative changes vs control (corrected for RpS9). The bars represent the mean for each condition, with error bars representing the S.E.M and individual values plotted as symbols. ns = not significant, two-way ANOVA followed by Students t-test. B) Pathogen abundance (in colony forming units, CFUs, per fly) control and rapamycin-treated flies at 4h and 24h during the 2h infection period and at 24h and 72h post-infection. ND= no detectable colonies. The bars represent the mean for each condition, with error bars representing the S.E.M and individual values plotted as symbols.

Disease Models & Mechanisms • DMM • Accepted manuscript

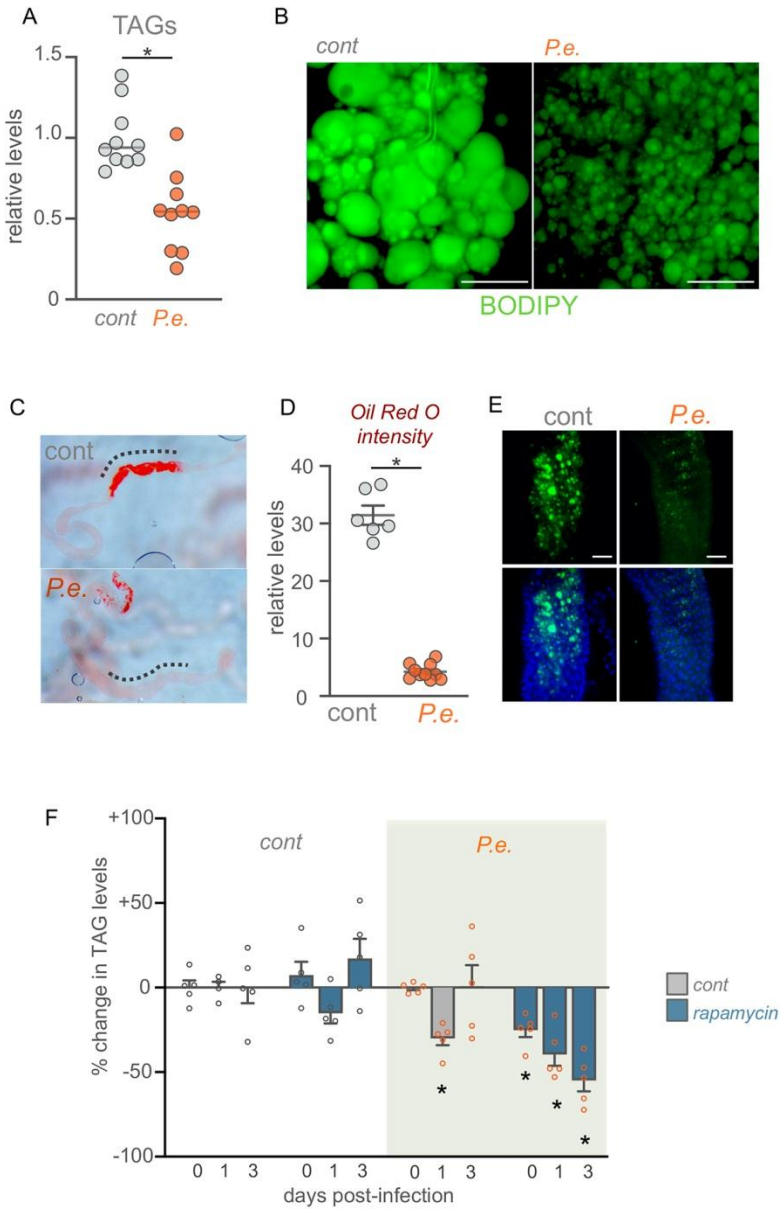

Figure 4. TOR signaling is required to limit excess lipid loss following enteric infection. A) Total TAG levels in control vs 48h *P.e* infected adults. Bars represent mean +/-SEM, individual data points are plotted as circles. *p<0.05, Students t-test. B) BODIPY staining of fat body of w^{1118} w^{1118}control and 24hr *P.e*. infected mated females. Green=BODIPY. Scale bar = 50 micrometres. N=5 animals per condition. C) Lipid droplet accumulation in the anterior region of the intestines stained with Oil- Red O (ORO) from control vs 24h *P.e* infected flies dye. High levels of lipid accumulation were seen in the anterior regions of control guts (indicated with dash line) and this was decreased in infected guts (N=10 per condition) D) ORO intensities in the anterior regions (indicated with dash line) of w^{1118} control and 24hr *P.e*. infected intestines. Bars represent mean +/-SEM, individual

Disease Models & Mechanisms • DMM • Accepted manuscript

data points are plotted as circles. . *p<0.05, Students t-test. E) BODIPY staining of anterior regions of w^{1118}control and 24hr *P.e*. infected intestines. Green=BODIPY, blue= Hoechst DNA dye. Scale bar = 50 micrometres. N+5 guts per condition. A representative image is shown. F) Adult w^{1118} mated females subjected to 24hr pre-treatment of rapamycin followed by 24hr oral *P.e.* feeding along with rapamycin. TAG assays were performed on flies at 0, 1 or 3 days after infection. The bars represent percentage change in TAG levels (compared to uninfected control animals), normalized to the protein content for each condition. The bars represent the mean for each condition, with error bars representing the S.E.M. and individual values plotted as symbols. * represents P <0.05 for each experimental group compared to the control group at the same timepoint.

Disease Models & Mechanisms • DMM • Accepted manuscript

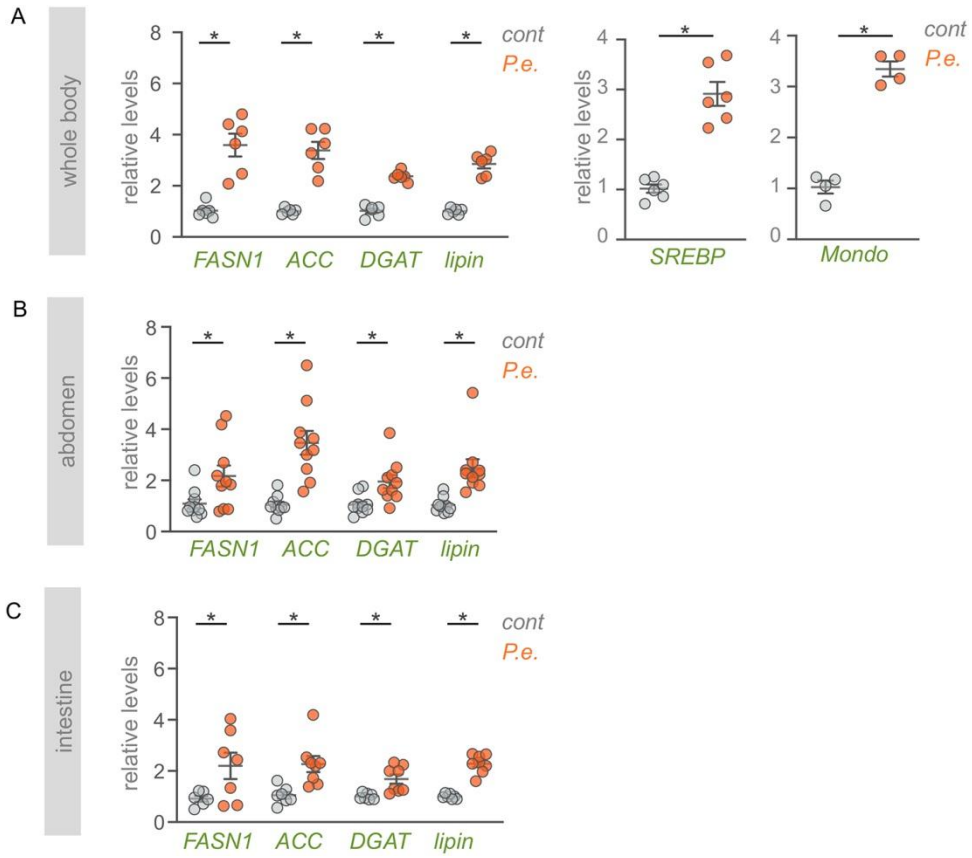

Figure 5. Enteric infection leads to increased expression of lipid synthesis genes in the intestine and abdominal fat. A) qPCR analysis from whole-body samples of control or *P.e.* infected flies of lipid synthesis genes (FASN1, ACC, DGAT and Lipin) and two transcription factors (SREBP and Mondo) that control the expression of lipid synthesis genes. Bars represent mean +/-SEM, individual data points are plotted as circles. *p<0.05, Students t-test. B) qPCR analysis of lipid synthesis genes from abdominal samples of control or *P.e.* infected flies. Bars represent mean +/-SEM, individual data points are plotted as circles. *p<0.05, Students t-test. C) qPCR analysis of lipid synthesis genes from intestinal samples of control or *P.e.* infected flies. Bars represent mean +/-SEM, individual data points are plotted as circles. *p<0.05, Students t-test.

Disease Models & Mechanisms • DMM • Accepted manuscript

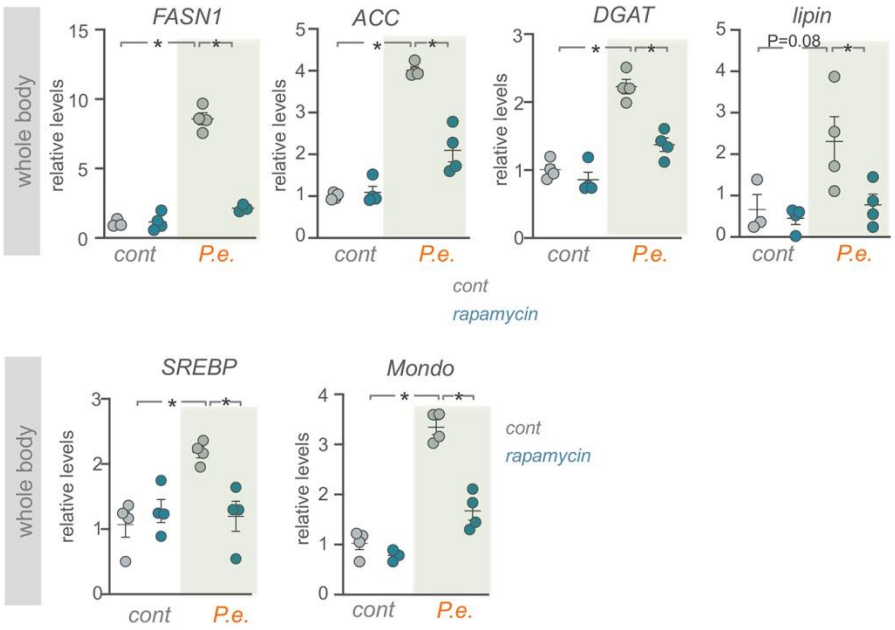

Figure 6. TOR is required for the increased expression of lipid synthesis genes induced by enteric infection. qPCR analysis of lipid synthesis genes and the transcription factors, SREBP and Mondo, in w^{1118} flies pretreated for 24h with either DMSO (control – grey symbols) or rapamycin (blue symbols), followed by 24h of either sucrose (control) or 24h oral *P.e.* feeding. Bars represent mean +/-SEM, individual data points are plotted as circles. * $p<0.05$, two-way ANOVA, followed by Students t-test.

Disease Models & Mechanisms • DMM • Accepted manuscript

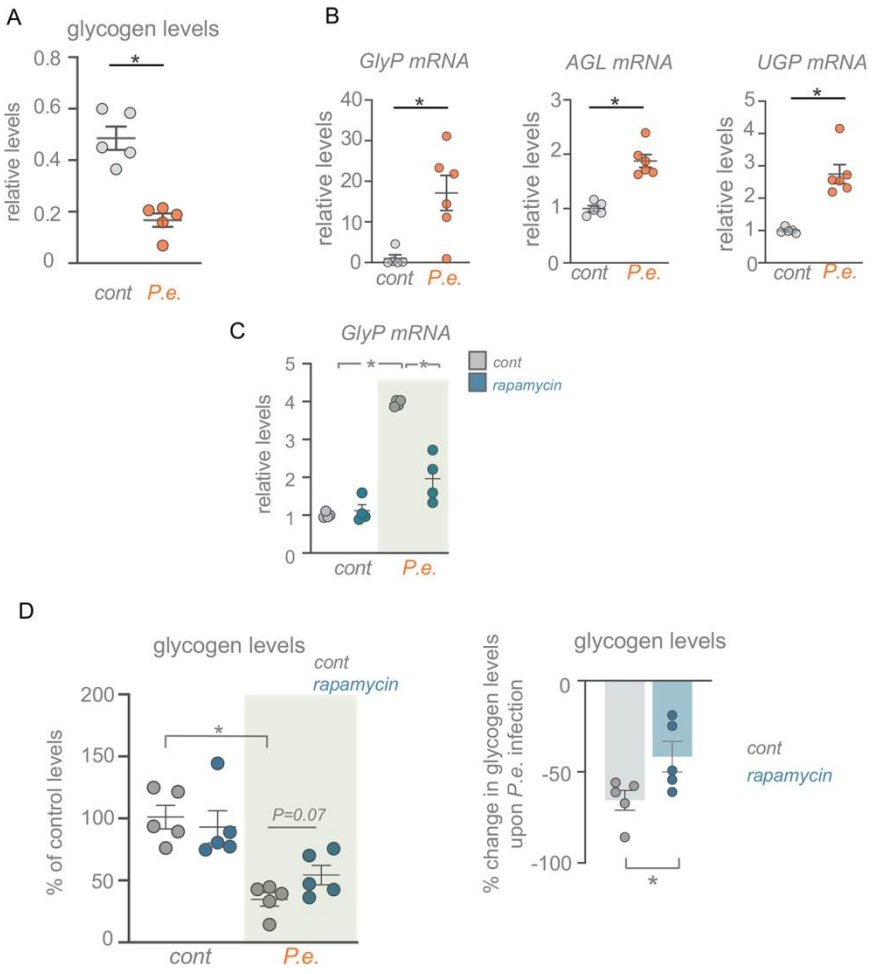

Figure 7. Enteric infection leads to glycogen mobilization in part through TOR activity.
Total glycogen levels in control vs 24hr *P.e* infected adults. Bars represent mean +/-SEM, individual data points are plotted as circles. *p<0.05, Students t-test. B) qPCR analysis of glycogen breakdown genes from whole-body samples of control or 24hr *P.e.* infected flies. Bars represent mean +/-SEM, individual data points are plotted as circles. *p<0.05, Students t-test. C) w^{1118} mated females were pretreated for 24 hours with either DMSO (control) or rapamycin, followed by 24hr of either sucrose (control) or 24hr oral *P.e.* feeding (grey bars). Whole animals were then processed for qRT-PCR analysis of GlyP mRNA. Bars represent mean +/-SEM, individual data points are plotted as circles. * p<0.05, two-way ANOVA, followed by Students t-test. D) w^{1118} mated females were pretreated for 24 hours with either DMSO (control) or rapamycin, followed by 24hr of either sucrose or 24hr oral *P.e.* feeding. Whole animals were then processed for measurement of total glycogen assays. Left, bars represent mean +/-SEM, individual data points are plotted as circles. *

Disease Models & Mechanisms • DMM • Accepted manuscript

p<0.05, two-way ANOVA, followed by Students t-test. Right, the data are presented as the percentage decrease in whole-body glycogen levels upon infection in control vs. rapamycin-treated samples. The bars represent the mean for each condition, with error bars representing the S.E.M. and individual values plotted as symbols. *p<0.05, Students t-test.

Disease Models & Mechanisms • DMM • Accepted manuscript

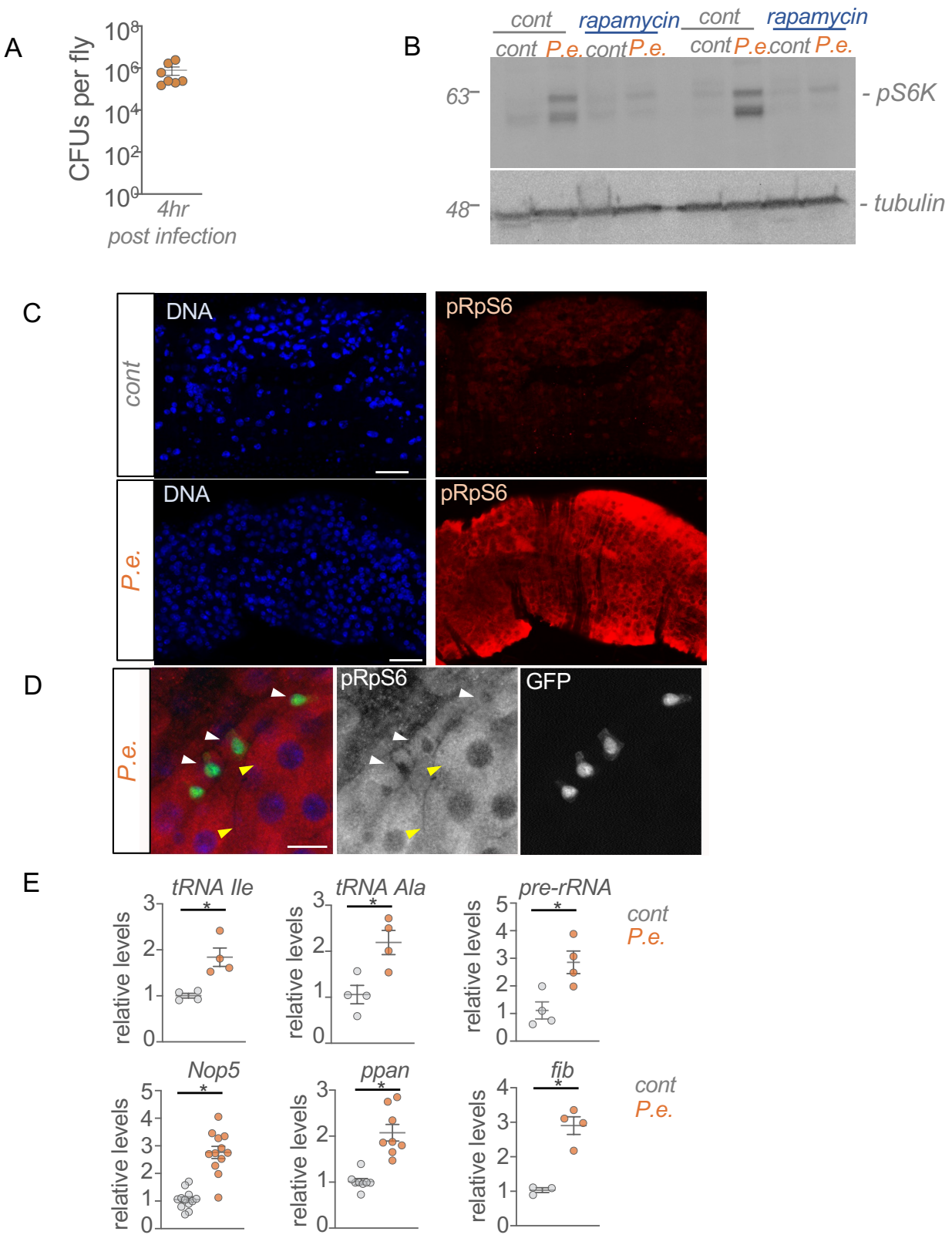

Fig. S1 (related to Figure 1). Infection with *P.e.* stimulates TOR activity in adult intestines. A) Pathogen abundance (in colony forming units, CFUs, per fly) at 4h following enteric *P.e.* infection. B) w^{1118} females were pretreated for 24 hours with either DMSO (cont) or rapamycin, followed by 4hr of either sucrose (cont) or 4hr *P.e.* feeding (grey bars). Intestinal samples were analyzed by western blot using antibodies to phosphorylated S6K and actin (as a loading control). C) Phosphorylated RpS6 (pRpS6) immunostaining in control vs 4hr *P.e.* infected flies. Blue, DNA; Red, anti-phospho RpS6 staining. Scale bar = 50 micrometres. Increased phospho S6 levels were observed in 10 out of 10 infected guts analyzed. D) Phosphorylated RpS6 (pRpS6) immunostaining in control vs 4hr *P.e.* infected flies. Blue, DNA; Red, anti-phospho RpS6 staining; Green, GFP positive ISC/EB cells marked by *esgGal4, UAS-GFP* (white arrowheads). Yellow arrowheads indicate large polyploid enterocytes. Scale bar = 10 micrometres. E) qPCR analysis of tRNA, pre-rRNA and ribosome synthesis genes from intestinal samples of control or 4hr *P.e.* infected flies. Bars represent mean +/-SEM, individual data points are plotted as circles. *p<0.05, Students t-test.

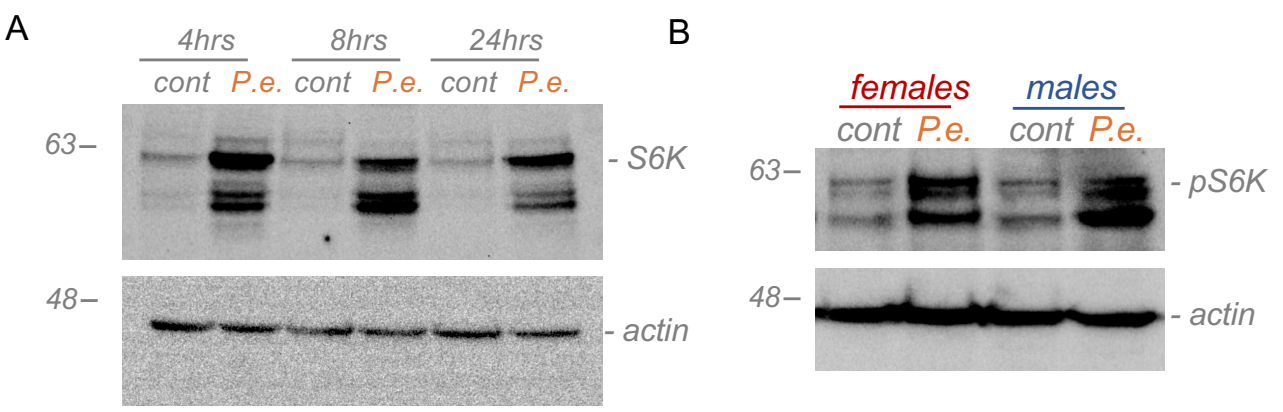

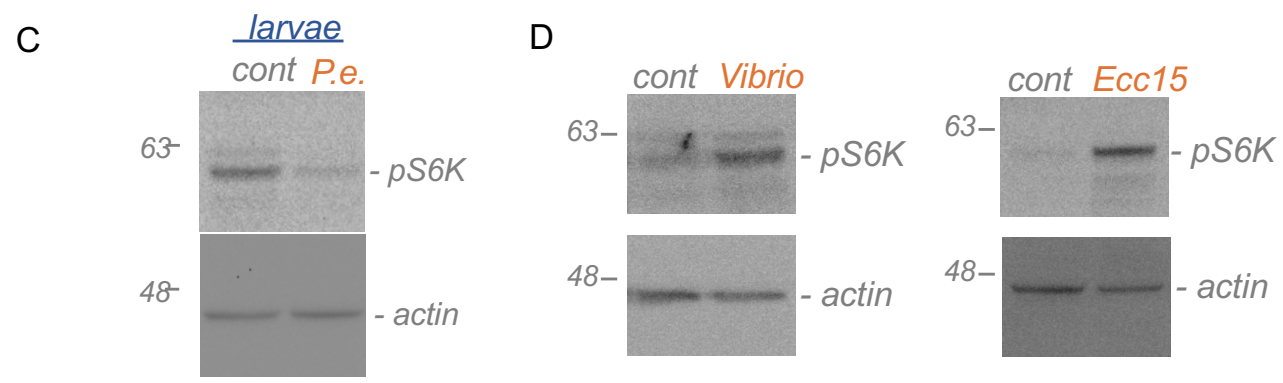

Fig. S2 (related to Figure 1). Enteric bacterial infection stimulates TOR activity in adult male and female intestines. A) Time course of *P.e.* infection on phosphorylated-S6K levels in intestines of w^{1118} mated females. Dissected intestines were analysed by western blotting using antibodies against phosphorylated-S6K and actin (loading control). B) Western blots of intestines from adult male and female flies subjected to 4hr oral *P.e* infection. Antibodies were against phosphorylated S6K (pS6K) and actin (loading control). C) Western blots of intestines from third instar larvae subjected to 4hr oral *P.e* infection. Antibodies were against phosphorylated S6K (pS6K) and actin (loading control). D) Western blots of intestines from adult flies subjected to 4hr oral infection with *V. Cholera* or *Ecc15*. Antibodies were against phosphorylated S6K (pS6K) and actin (loading control).

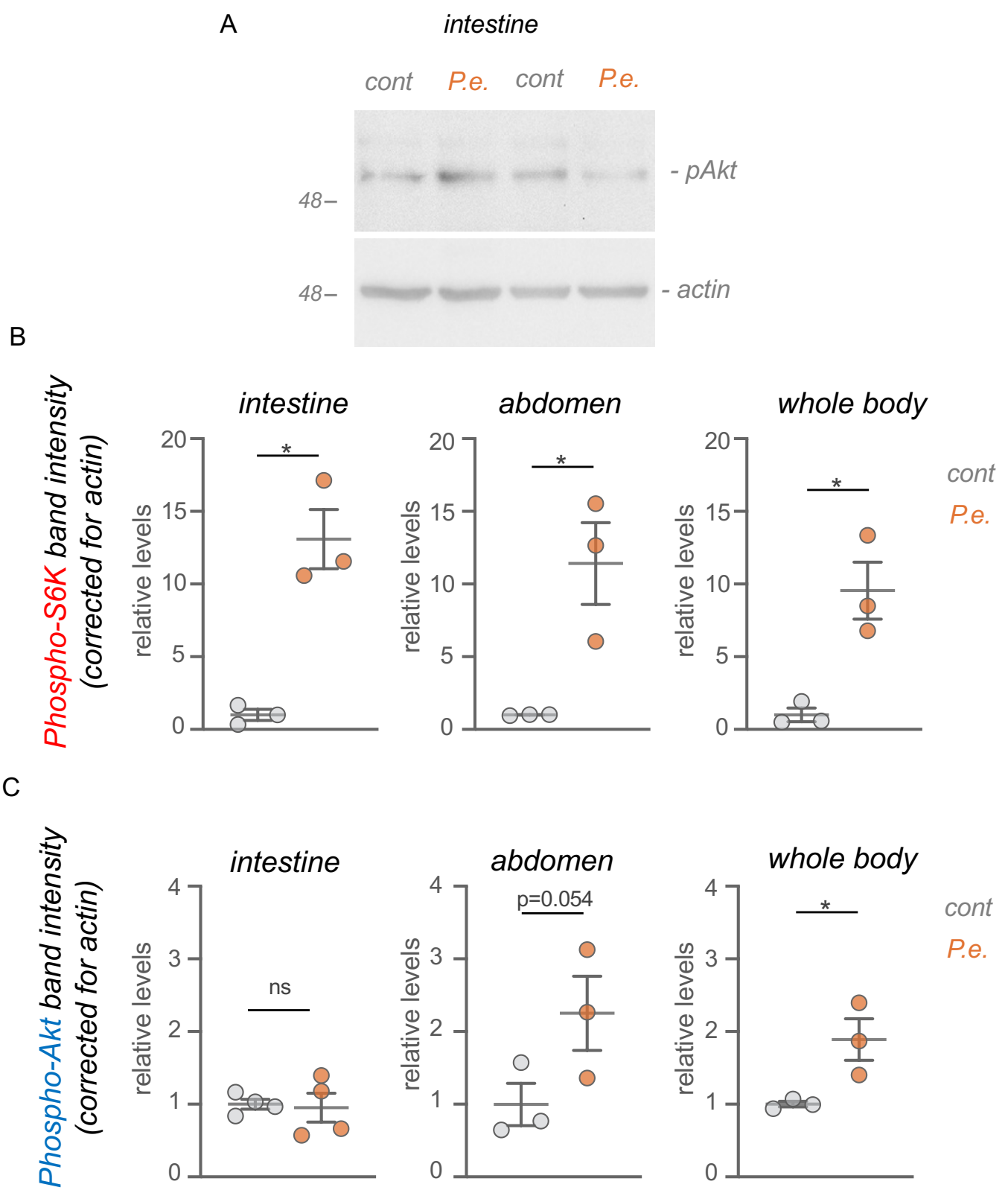

Fig. S3 (related to Figure 1). Enteric bacterial infection effects on S6K and Akt phosphorylation in the intestine, abdomen and whole-body. A) Western blots of intestinal samples from adult flies subjected to 4hr oral *P.e* infection using antibodies to phosphorylated Akt, (pAkt) and actin (as a loading control). B, C) Quantification of B) phosphoS6K and C) phosphoAkt, western blots of intestinal, abdominal and whole-body samples from adult flies subjected to 4hr oral *P.e* infection. Band intensities were corrected for actin levels. Bars represent mean +/-SEM, individual data points are plotted as circles. *p<0.05, ns= not significant, Students t-test.

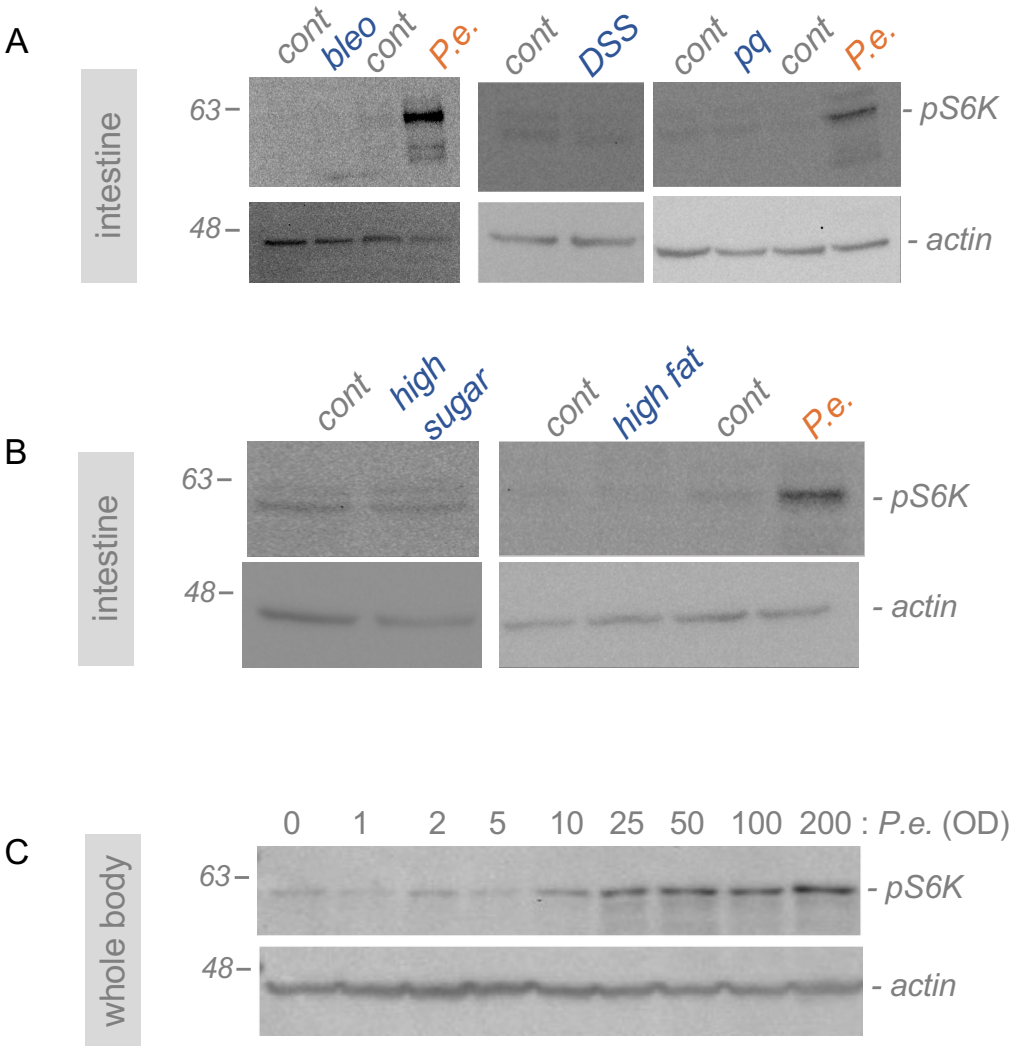

Fig. S4 (related to Figure 1). Enteric bacterial infection, but not other environmental stress, stimulates TOR activity in the intestine. A) Western blot of dissected intestines from adult flies subjected to 4hr treatments of chemical stressors: 25μg/ml Bleomycin, 5% DSS, 2mM paraquat. Antibodies were against phosphorylated S6K (pS6K) and actin (loading control). B) Western blot of dissected intestines from adult flies subjected to 4hr feeding with high sugar (40% sucrose), high fat (30% lard) or *P.e.* Antibodies were against phosphorylated S6K (pS6K) and actin (loading control). C) Western blot of whole-body samples from adult flies subjected to 4hr feeding with different concentrations (OD_{600} 1-200) of *P.e.* Antibodies were against phosphorylated S6K (pS6K) and actin (loading control).

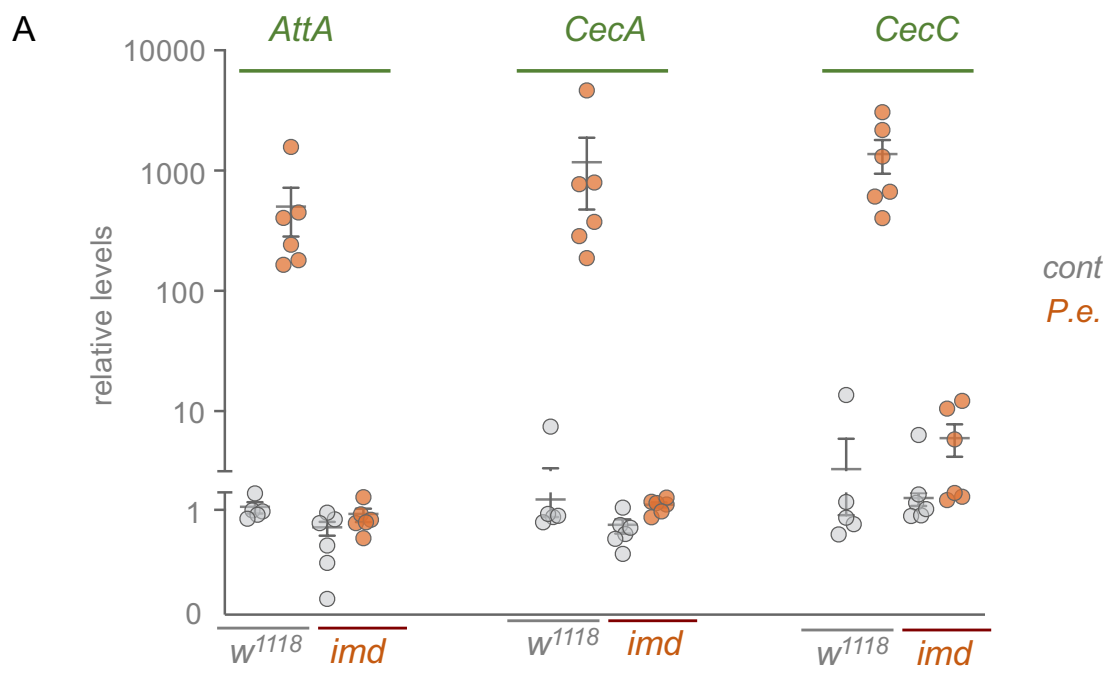

Fig. S5 (related to Figure 2). AMP induction is blocked in *imd* mutants. qPCR analysis of AMP genes from whole-body samples of w^{1118} or *imd* mutant animals following 24hr of *P.e.* infection. Bars represent mean +/-SEM, individual data points are plotted as circles.

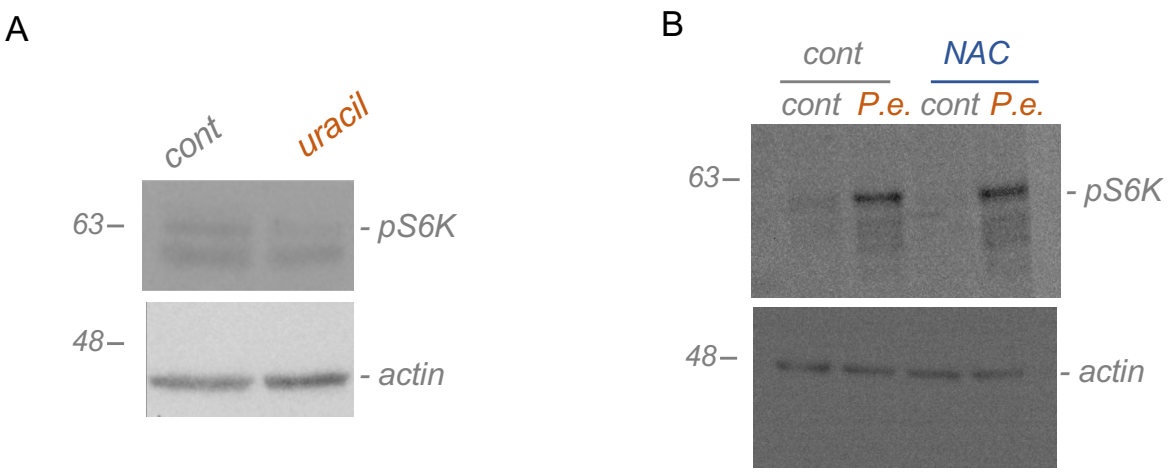

Fig. S6 (related to Figure 2). Uracil or ROS are not involved in TOR induction. A) Western blot of dissected intestines from adult control vs 4hr uracil-fed flies. Antibodies were against phosphorylated S6K (pS6K) and actin (loading control). B) Western blot of dissected intestines from adult control vs 4hr *P.e.* infected flies that had been pretreated for 2 days with either water (control) or N-acetyl cysteine (NAC). Antibodies were against phosphorylated S6K (pS6K) and actin (loading control).

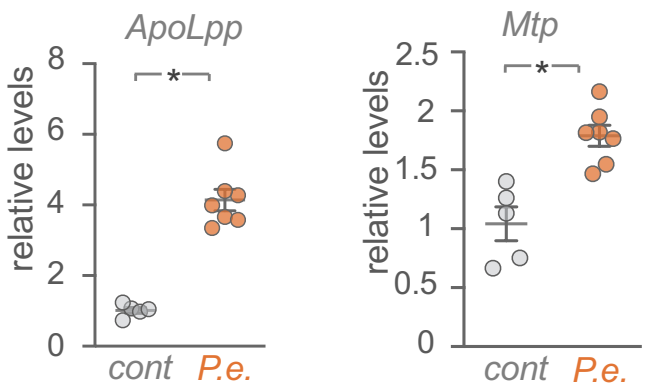

Fig. S7 (related to Figure 4). Enteric infection increases the expression of apolipoprotein mRNAs. qPCR analysis of *ApoLpp* or *Mtp* from whole-body samples of *control vs* 24hr infected *P.e.* animals. Bars represent mean +/-SEM, individual data points are plotted as circles.

Disease Models & Mechanisms • Supplementary information

Table S1. A list of primers used in this study

Gene name	Forward sequence	Reverse sequence
Fatty acid synthetase 1(CG3523) (FASN1)	TCCCAGAGGCAAACATTACC	TCGGGGAAATGAAGAAGATG
Acetyl-CoA carboxylase (CG11198) (ACC)	GCCAAGAGCATAACGAGGAG	GCTCCAGATGCCGGTAAATA
Midway (DGAT)	CTCTTTAGTGCATATCTCGCTCTG	AACAAGCCCAAGCCCTCT
lipin	CTCGGCGGCTATCAAAA	ACCTTGTCGTTGTGCTTCCA
Lipid storage droplet (LSD)-2	AGAGCAAGGTGATCGATGTG	ACTCCGTTGACAGCCAGACT
Mondo	GCGGCGTTACAACATAAAGA	CTCCATGCGCAAAGCTTCAA
SREBP	AAGGACACTCTCTGGGCTGA	GCTTGATCCTGCCGTACAAT
GlyP	CAACTGGTTGCTCTGAAGAAGTG G	CTGGCGCTTGTACTCGTGAATACG
tRNA Ala	GCGGCCGCACTTTCACTGACCGGA A ACG	GCGGCCGCGCCCGTTCTAACTTTTT GGA
tRNA Ile	CGACCTTCGCGTTATTAGCA	GGCCCATTAGCTCAGTTGGT
tRNA Arg	GCGGCCGCGTCCGTCCACCAATG AA AAT	GCGGCCGCCGGCTAGCTCAGTCGG T AGA
Diptericin	GGCTTATCCGATGCCCGACG	TCTGTAGGTGTAGGTGCTTCCC
Attacin A	AGGAGGCCCATGCCAATTTA	CATTCCGCTGGAACTCGAAA
Cecropin A	TCTTCGTTTTCGTCGCTCTCA	ATTCCCAGTCCCTGGATTGTG

Disease Models & Mechanisms • Supplementary information

Cecropin C	TCATCCTGGCCATCAGCATT	CGCAATTCCCAGTCCTTGAAT
Drosocin	TTTGTCCACCACTCCAAGCAC	ATGGCAGCTTGAGTCAGGTGA
Metchnikowin	CGATTTTTCTGGCCCTGCT	CCGGTCTTGGTTGGTTAGGAT
Act5C	GAGCGCGGTTACTCTTTCAC	ACTTCTCCAACGAGGAGCTG
RpS9	AAACCTGCTCGGTTGAATTG	TTGTTGCGCAGACCATACTC
5S RNA	ACGACCATACCACGCTGAAT	AGCGGTCCCCCATCTAAGTA

Disease Models & Mechanisms • Supplementary information